Provenance and tectonic significance of the Palaeoproterozoic metasedimentary successions of central and northern Madagascar

B. De Waele [a,b,∗], R.J. Thomas [b], P.H. Macey [c], M.S.A. Horstwood [b], R.D. Tucker [e], P.E.J. Pitfield [b], D.I. Schofield [b], K.M. Goodenough [d], W. Bauer [b], R.M. Key [d], C.J. Potter [e], R.A. Armstrong [f], J.A. Miller [g], T. Randriamananjara [h], V. Ralison [h], J.M. Rafahatelo [h], M. Rabarimanana [h], M. Bejoma [i]

[a] SRK Consulting, Level 1, 10 Richardson Street, West Perth, WA 6005, Australia
[b] British Geological Survey, Keyworth, Notts NG12 5GG, United Kingdom
[c] Council for Geoscience, Western Cape, South Africa
[d] British Geological Survey, Murchison House, Edinburgh, United Kingdom
[e] United States Geological Survey, Reston, VA 20192, USA
[f] Australian NationalUniversity, Canberra, Australia
[g] Stellenbosch University, Stellenbosch, South Africa
[h] Projet de Gouvernance des Ressources Minières, Antananarivo, Madagascar
[i] Université de Antananarivo, Antananarivo, Madagascar

ARTICLE INFO

ABSTRACT

New detrital zircon U–Pb age data obtained from various quartzite units of three spatially separated supracrustal packages in central and northern Madagascar, show that these units were deposited between 1.8 and 0.8 Ga and have similar aged provenances. The distribution of detrital zircon ages indicates an overwhelming contribution of sources with ages between 2.5 and 1.8 Ga. Possible source rocks with an age of 2.5 Ga are present in abundance in the crustal segments (Antananarivo, Antongil and Masora Domains) either side of a purported Neoproterozoic suture ("Betsimisaraka Suture Zone"). Recently, possible source rocks for the 1.8 Ga age peak have been recognised in southern Madagascar. All three supracrustal successions, as well as the Archaean blocks onto which they were emplaced, are intruded by mid-Neoproterozoic magmatic suites placing a minimum age on their deposition. The similarities in detrital pattern, maximum and minimum age of deposition in the three successions, lend some support to a model in which all of Madagascar's Archaean blocks form a coherent crustal entity (the Greater Dharwar Craton), rather than an amalgamate of disparate crustal blocks brought together only during Neoproterozoic convergence. However, potential source terranes exist outside Madagascar and on either side of the Neoproterozoic sutures, so that a model including a Neoproterozoic suture in Madagascar cannot be dispelled outright.

© 2011 Elsevier B.V. All rights reserved.

1. Introduction

Madagascar occupies a critical, central position within the East African Orogen (EAO; Fig. 1). Consequently, an understanding of the geological history of its component terranes is important for constraining the palaeogeography of the entire region through time and elucidating the assembly history of Gondwana. Many recent studies of the geology of Madagascar have focused on comparisons between the three component Archaean cratonic domains and intervening paragneiss assemblages (Collins, 2006 and references therein). However, new data have been obtained for the northern half of Madagascar through a concerted phase of geological mapping and research undertaken by teams from the British and United States Geological Surveys (BGS-USGS) and the Council for Geoscience of South Africa (CGS), in conjunction with Malagasy geologists from the *Projet du Governance des Ressources Minérales* (PGRM), as part of a multi-disciplinary, World Bank-sponsored project which ran between 2004 and 2008 (see BGS-USGS-GLW, 2008 and CGS, 2009a,b). This study facilitated re-interpretations of the tectonic framework of the northern half of Madagascar. In this paper we focus on a poorly understood aspect of the Precambrian shield: the age and provenance of the enigmatic metasedimentary units of Proterozoic age that rest upon the Archaean cratons of central and eastern Madagascar.

∗ Corresponding author at: SRK Consulting, Level 1, 10 Richardson Street, West Perth, WA 6005, Australia.
E-mail addresses: bdewaele@srk.com.au, info@bdewaele.be (B. De Waele).
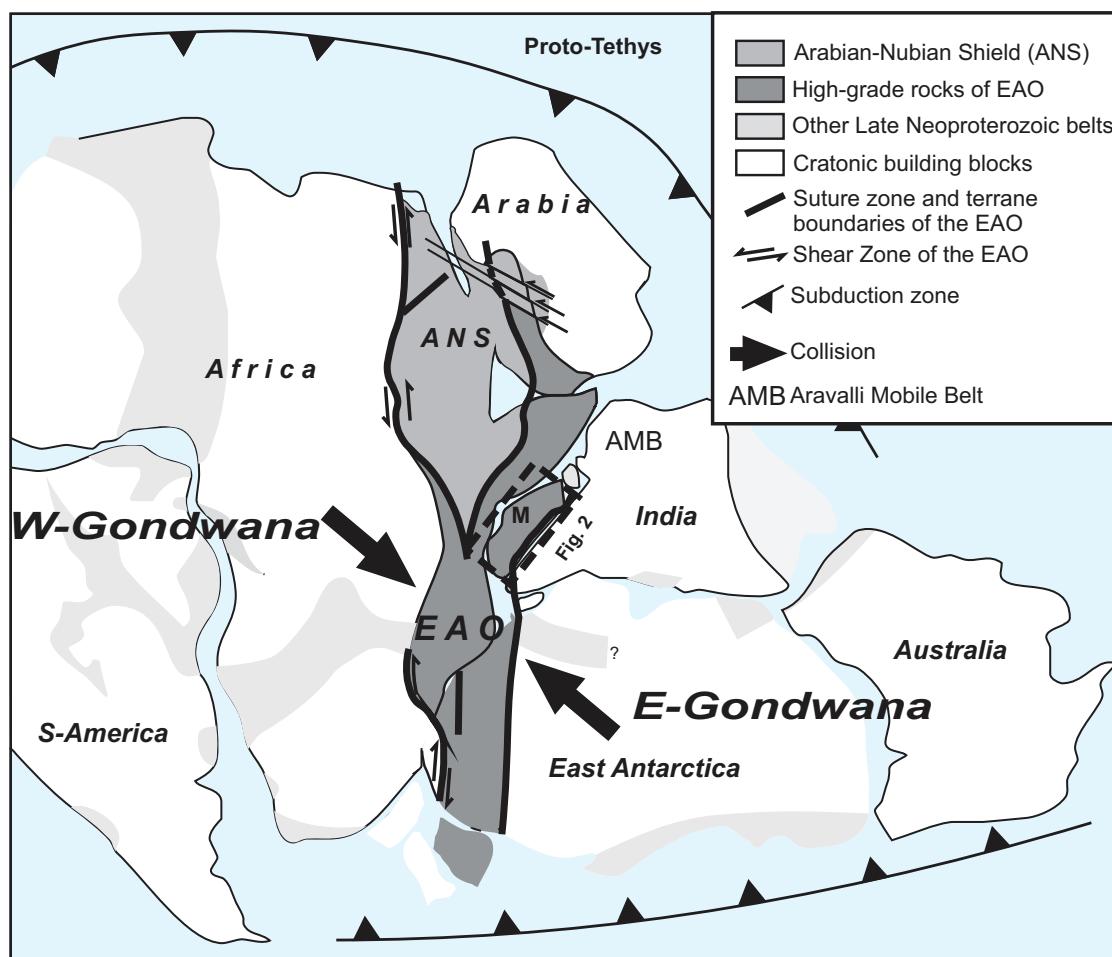
Fig. 1. Palaeoposition of Madagascar in Gondwana (after Thomas et al., 2009).

The ancient shield of Madagascar is composed of distinctive Archaean crustal blocks: the dominantly Meso- to Neoarchaean blocks of east Madagascar (Antongil and Masora cratons) and the exclusively Neoarchaean block of central Madagascar (Antananarivo Craton, Fig. 2). Two very different hypotheses attempt to explain their present-day juxtaposition. A widely-accepted hypothesis (e.g. Collins, 2006 and references therein) portrays them as disparate fragments of peninsular India and central East Africa, respectively, joined along a convergent margin boundary – the "Betsimisaraka suture" – active throughout Neoproterozoic time (ca. 800–550 Ma). The "Betsimisaraka suture" comprises a belt of Neoproterozoic metasedimentary rocks, intruded by voluminous Neoproterozoic to Cambrian granitoids, which has been named as the Anaboriana-Manampotsy belt (Fig. 2). Another hypothesis (Tucker et al., 2010a,b) portrays them as different parts of a common craton (the Greater Dharwar Craton) joined by a Neoarchaean accretion event (ca. 2.5 Ga). Both perspectives acknowledge that the disparate Archaean cratons are overlain by metasedimentary rocks of Proterozoic age: the eastern Antongil and Masora cratons by the Sahantaha and Maha groups respectively, and the western Antananarivo Craton by the Itremo Group (Fig. 2). The metasedimentary rocks represent either remnants of discrete sedimentary basins deposited on the Archaean cratons, and/or dissected parts of one or more parautochthonous to allochthonous sheets that were structurally emplaced during post-depositional orogenic events (e.g. De Waele et al., 2008).

Of the three successions described here, the Itremo Group, which locally overlies the western Antananarivo Craton, is the best-studied (Figs. 2, 3). It comprises a thick succession of quartzite, metapelite and metacarbonate, affected by (sub-)greenschist facies metamorphism, and has yielded detrital zircon age data with the largest modes at ca. 2500 and 1850 Ma (Cox et al., 1998, 2004a; Fitzsimons and Hulscher, 2005). On the basis of the geochronological data, carbonate δ^{13}C compositions and the morphology of stromatolites in the succession, the Itremo Group is regarded as having been deposited during the Late Palaeoproterozoic (Cox et al., 1998, 2004a; Fitzsimons and Hulscher, 2005), although a younger age cannot be ruled out. As yet, bedrock of Palaeoproterozoic age (ca. 2.0–1.8 Ga) has only been identified in southern Madagascar (Tucker et al., 2010a). Nevertheless, a close match of detrital zircon ages from the Itremo Group with the Ubendian-Usagaran belts of east Africa (e.g. marginal to the Tanzania Craton), led Cox et al. (1998, 2004a) and Fitzsimons and Hulscher (2005) to conclude that the Antananarivo Craton was derived from East Africa. In their view, the Itremo Group was deposited unconformably on the East African margin, and a piece of it (the future Antananarivo Craton) rifted away to form a microcontinent, "Azania" (Collins and Pisarevsky, 2005). The Antananarivo Craton and overlying supracrustal rocks were then metamorphosed and deformed during an early Neoproterozoic orogenesis (ca. pre-800 Ma, Collins et al., 2003b; Collins, 2006) prior to its rifting away, and subsequent amalgamation with east Madagascar.
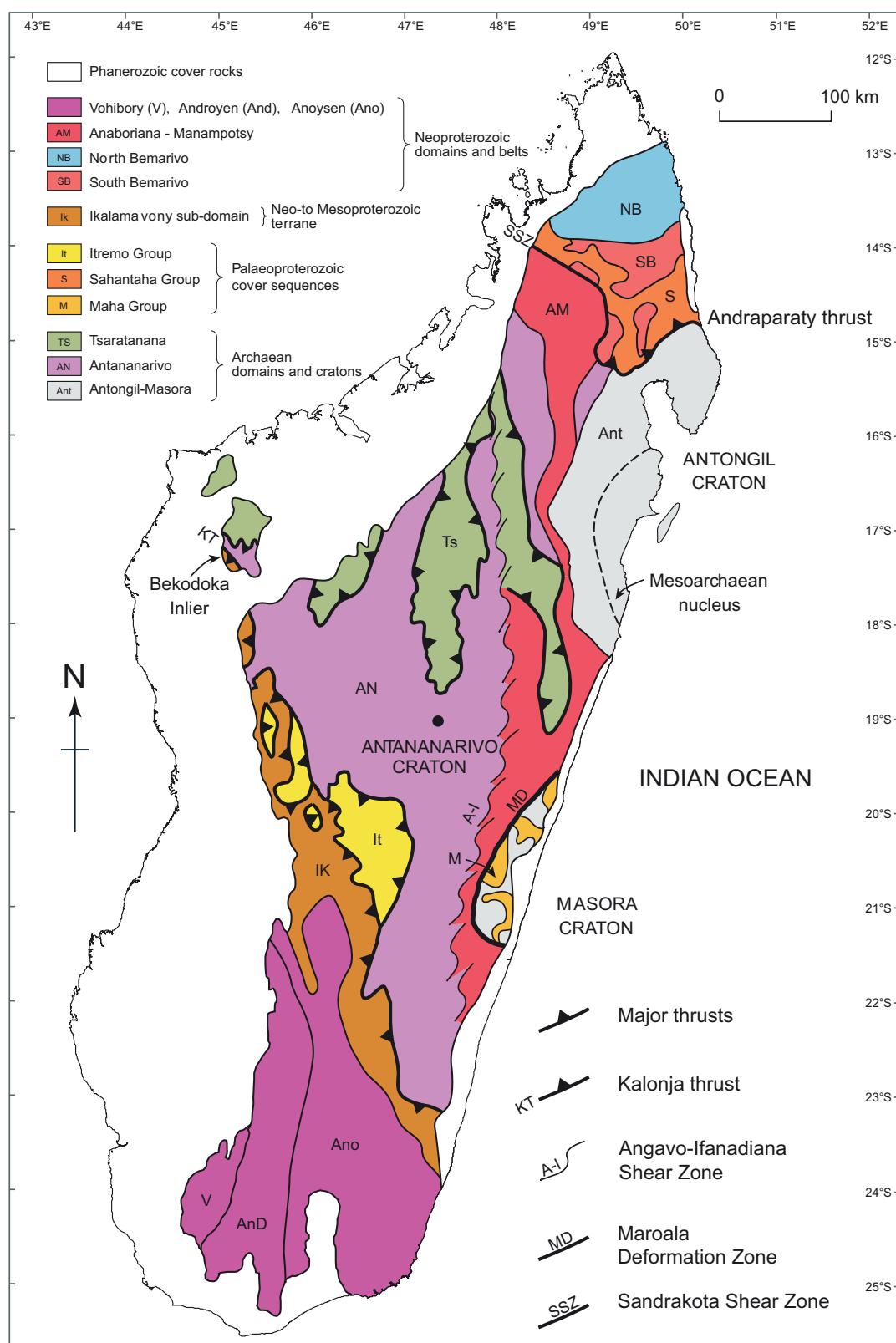
Fig. 2. Tectonic architecture of Madagascar showing the location of successions described in the text.

The less well-studied Sahantaha Group of northern Madagascar has been variably metamorphosed up to amphibolite-/granulite-facies, in contrast to the dominant greenschist metamorphism in the Itremo and Maha groups. Two samples of quartzite of the Sahan-taha Group yielded a U–Pb detrital zircon signature comparable to the Itremo Group (Cox et al., 2003).

In this paper, we compare and contrast the lithostratigraphic, metamorphic and structural characteristics of the three groups, and
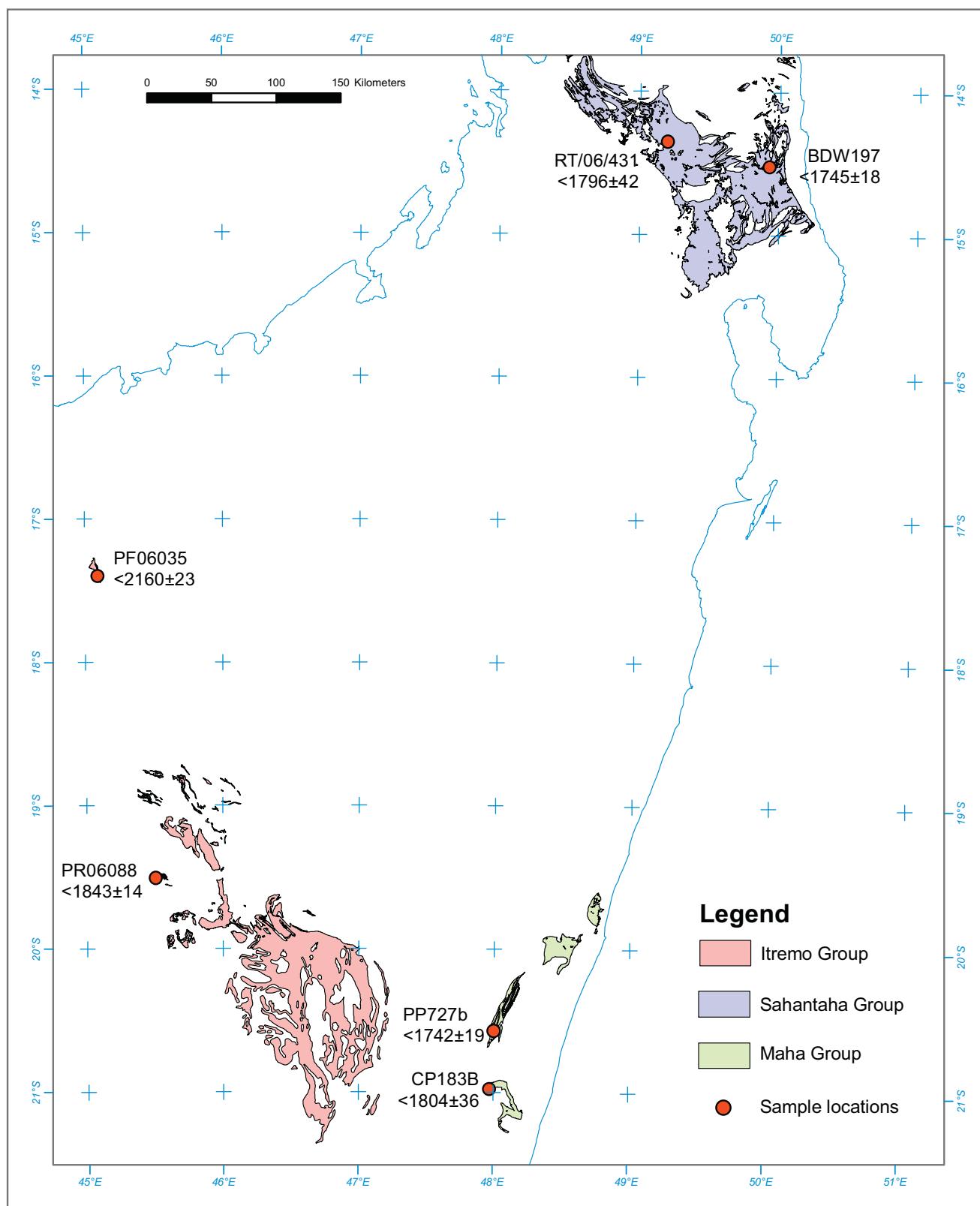
Fig. 3. Distribution of the Itremo, Sahantaha and Maha groups and location of the geochronological samples.

present further detrital zircon age data on the Itremo Group, along with new detrital age data for the Sahantaha and Maha groups, which overlie the Antongil and Masora cratons respectively. On the strength of these data, we re-examine existing models for the post-Archaean (Pan-African) tectonic development of Madagascar.

2. Geology of the tectonic terranes

The recent phase of 1:100,000 to 1:500,000 scale geological mapping has allowed the redefinition of the various tectonic terranes of central and northern Madagascar (BGS-USGS-GLW, 2008;

CGS, 2009a,b, see Fig. 2), the salient features of which are briefly described below:

2.1. Antongil Craton

This terrane of NE Madagascar dominantly comprises of granitoids of two main ages. An older Mesoarchaean nucleus, centred on the island of Nosy Boraha (Isle de Saint Marie) is characterised by intrusive TTG gneisses and supracrustal rocks (Nosy Boraha Suite and Fenerivo Group) dated at ca. 3.32–3.18 Ga (Tucker et al., 1999, 2010a). Intrusive into these are voluminous Neoarchaean (ca. 2.54–2.50 Ga) granitoids (Masoala Suite, Tucker et al., 1999, 2010b; Paquette et al., 2003; Schofield et al., 2010) and related supracrustal rocks of the Mananara Group (Schofield et al., 2010). The Masoala Suite, which constitutes over 90% by area of the northern Antongil Craton, is composed of a wide range of migmatitic granitoid lithologies of late Neoarchaean age, with minor disrupted mafic schist and paragneiss bodies of the Mananara Group occurring as xenolithic pods, lenses and schlieren (Schofield et al., 2010). In the northern Antongil Craton, a widespread suite of metagabbro/microgabbro intrusions known as the Ankavanana Suite, as well as a minor supracrustal succession of limited extent and ascribed to the Andrarona Group have been shown to be Palaeoproterozoic in age (Schofield et al., 2010). The Antongil Craton largely escaped Neoproterozoic reworking.

2.2. Masora Craton

The Masora Craton comprises TTG orthogneisses of the Befody Suite (3.3–3.1 Ga; BGS-USGS-GLW, 2008; Tucker et al., 2010b), which are correlated with the Nosy Boraha Suite of the Antongil Craton. Supracrustal units form an important component of the Masora Craton and include the dominantly greenschist-grade metasedimentary and metavolcanic Maha Group, and the amphibolite-grade metamafite-paragneiss-paraschist-banded iron formation-serpentinised ultramafic pods association of the Vohilava Group. Thus the Vohilava Group has a metavolcani-clastic character (paragneiss, schist and amphibolites) and could be a possible correlative to the Meso- to Neoarchaean Mananara Group in the Antongil Craton. In general, the Masora Craton rocks show early amphibolite facies metamorphism with some late high-temperature ductile shearing and a more widespread low greenschist facies overprint.

The Masora Craton differs from the Antongil Craton by the apparent absence of Neoarchaean felsic magmatism, a greater proportion of supracrustal units and by widespread Neoproterozoic reworking. The southern and western margins of the Masora Craton are juxtaposed against the Neoproterozoic Anaboriana-Manampotsy Belt along the curviplanar "Maroala Deformation Zone" (MD, Fig. 2), comprising a tectonically mixed package of continental margin sedimentary rocks and Masora Craton rocks. 840–760 Ma granites-granodiorites, leucotonalites to quartz diorites and metagabbro-diorites occur throughout the Masora Craton mostly as folded sheets; ca. 630 Ma granites are localised within the MD and the adjacent Anaboriana-Manampotsy Belt (BGS-USGS-GLW, 2008).

2.3. Antananarivo Craton

The Antananarivo Craton consists of Archaean orthogneisses (Betsiboka Suite), which record zircon U–Pb ages of 2.5 Ga (see for instance Kröner et al., 2000; Tucker et al., 2007 and BGS-USGS-GLW, 2008) and paragneisses (Vondrozo and Sofia groups) that were metamorphosed and partially melted under granulite- and upper amphibolite-facies conditions in Neoarchaean time (Nicollet, 1990; Goncalves et al., 2004; BGS-USGS-GLW 2008;

CGS, 2009a; Tucker et al., 2010a). The age evidence includes SHRIMP and Pb–Pb evaporation dates obtained on deformed granulites (2747–2515 Ma, Kröner et al., 2000) and Thermal Ionisation Mass Spectrometry (TIMS) studies on four samples south of Antananarivo (2590–2503 Ma, Tucker et al., 1999). Indications for Palaeoproterozoic and Mesoproterozoic crust incorporated within the Antananarivo Craton include zircon xenocrysts retrieved from Neoproterozoic intrusions with ages from 2188 to 1007 Ma (three between 1057 and 1007 Ma, Kröner et al., 2000), but those could also have been derived from metasedimentary rocks.

A series of structurally overlying, possibly allochthonous belts of predominantly mafic gneisses occur within the Antananarivo Craton, collectively termed the Tsaratanana Complex (Collins et al., 2003a; BGS-USGS-GLW, 2008; CGS, 2009b). These comprise, from west to east, the Ambohipaky, Maevatanana, Andriamena, and Beforona-Alaotra belts (Fig. 2). They are composed of mafic tonalitic orthogneisses and paragneiss sequences of Archaean age (Tucker et al., 1999, 2007; Goncalves et al., 2003, 2004; CGS, 2009b). Field evidence from the basal contact of the Beforona-Alaotra Belt, which overlies the mid-Neoproterozoic Anaboriana-Manampotsy Belt, suggests tectonic juxtapositioning with the underlying Antananarivo Craton, although this structural inversion could have resulted from recumbent and overturned folding.

Large volumes of magma were intruded throughout the Antananarivo Craton – Tsaratanana Complex as a result of Neoproterozoic to Cambrian orogenesis during three major episodes, the Imorona-Itsindro, Kiangara and Ambalavao-Maevarano intrusive events:

(a) The Imorona-Itsindro magmatism occurred between 855 and 720 Ma (maximum range that also includes Pb–Pb evaporation data, Kröner et al., 2000; CGS, 2009a,b; BGS-USGS-GLW, 2008). The Imorona-Itsindro Suite comprises variably deformed syenites, gabbros (Handke et al., 1997a,b, 1999; Tucker et al., 1999, 2007; CGS, 2009a,b) and granitoids (Kröner et al., 2000; Collins et al., 2003b);

(b) The Kiangara Suite is dated at between 634 and 565 Ma (Ashwal, 1997; Paquette and Nédélec, 1998; Kröner et al., 1999a,b, 2000; Tucker et al., 1999, 2007; Meert et al., 2001; CGS, 2009a) and comprises thick (<0.5 km) sill-like intrusions known in the literature as "granitoïdes stratoïdes" (Meert et al., 2003; BGS-USGS-GLW, 2008).

(c) The Ambalavao-Maevarano suites comprises largely post-tectonic granitoids with an age range of 565–520 Ma (e.g. Meert et al., 2003; Goodenough et al., 2010 and references therein).

The Antananarivo Craton is juxtaposed against the Antongil and Masora cratons along a system of steeply-dipping high strain zones incorporating intercalated units of younger (Neoproterozoic) sedimentary and igneous rocks that form part of the Anaboriana-Manampotsy Belt (BGS-USGS-GLW, 2008). This belt of high-grade Neoproterozoic metasedimentary rocks and orthogneisses is broadly, but not exactly, spatially coincident with the 'Betsimisaraka Suture Zone' as proposed by Kröner et al. (2000). Previous workers suggested that the Antongil/Masora and Antananarivo cratons were separated by an oceanic tract prior to collision and the amalgamation of Gondwana (e.g. Collins et al., 2000a; Kröner et al., 2000; Collins, 2006 and references therein). In support of this contention, there are very distinct lithological and structural differences between the rock assemblages of the Antongil, Masora and Antananarivo cratons showing that they represent lithologically/rheologically discrete fragments of Archaean crust (Raharimahefa and Kusky, 2009). Other workers dispute the presence of a suture and favour a model of a contiguous Archaean "Greater Dharwar" craton (e.g. Tucker et al., 2010a,b). BGS-USGS-GLW (2008) suggest a more complex history of Neoproterozoic-Cambrian Pan-African orogenesis

involving initial amalgamation of the Antananarivo and Masora cratons across the Anaboriana-Manampotsy Belt between about 820 and 740 Ma. Later (ca. 560 Ma) collision of the Antongil Craton with the amalgamated Antananarivo-Masora cratons took place across the Anaboriana Domain of the Anaboriana-Manampotsy Belt (Goodenough et al., 2010).

2.4. Bemarivo Belt

The Bemarivo Belt consists of juvenile magmatic arc crust (Tucker et al., 1999; Thomas et al., 2009) and associated arc-volcanosedimentary rocks that were accreted to the northern edge of Madagascar at ca. 520 Ma (Buchwaldt and Tucker, 2001; Buchwaldt et al., 2002, 2003; Buchwaldt, 2006; Jöns et al., 2005a,b, 2006; Thomas et al., 2009). The belt is composed of two arc terranes (Thomas et al., 2009), dated at ca. 750 Ma (Southern Bemarivo Domain) and ca. 720 Ma (Northern Bemarivo Domain, see Fig. 2). These amalgamated arc terranes were translated southward across a composite Archaean foreland, with a postulated Palaeoproterozoic infrastructure, along an imbricate décollement system termed the Andaparaty Thrust (see Fig. 2 and Thomas et al., 2009).

The southern, structurally lower part of the Bemarivo Belt is dominated by extensive metasedimentary rocks of the Sahantaha Group. Arc-related granitoid rocks, dated at ca 750 Ma and known as the Antsirabe North Suite, contain metasedimentary xenoliths which may be fragments of the Sahantaha Group (although this remains unproven). Intercalated metasedimentary successions in the northern Bemarivo Belt include the Betsiaka Group, limited to a narrow strip along the northwestern edge of the terrane, which gave detrital zircon ages no younger than ca. 2450 Ma and two much younger volcano-sedimentary successions, the Milanoa and Daraina groups, directly dated at 749–720 Ma (Tucker et al., 1999) with detrital zircon ages of 770–720 Ma (Thomas et al., 2009). The Milanoa and Daraina groups have a notable lack of older detrital age components, testifying to their juvenile Neoproterozoic character.

2.5. Itremo-Ikalamavony Domain

The Itremo-Ikalamavony Domain (Fig. 2) is an Early Cambrian east-vergent fold-and-thrust belt comprising tectonically interleaved Proterozoic supracrustal and metaplutonic gneisses, translated eastwards with, and over, the reworked migmatitic rocks of the Antananarivo Domain (Moine, 1974; Fernandez et al., 2001, 2003; Fernandez and Schreurs, 2003; Nédélec et al., 2003; Cox et al., 2004b; Tucker et al., 2007, 2010a,b; CGS, 2009a,b; GAF-AG-BGR, 2009).

The domain is further subdivided into two sub-domains on the basis of differences in lithostratigraphy and metamorphic grade. In the east, the large nappes of the Itremo Sub-domain, or as it was formerly known the "Massif Schisto-Quartzo-Dolomitique" (SQD, Moine, 1974), are dominated by the Palaeoproterozoic greenschist and locally lower amphibolite facies metasedimentary rocks (quartzite, marble and pelite) of the Itremo Group that are intruded by, and tectonically interleaved with, mid-Neoproterozoic (~800 Ma) orthogneisses of the Imorona-Itsindro Suite (Moine, 1974; Fernandez and Schreurs, 2003; Cox et al., 2004b; Tucker et al., 2007; CGS, 2009a,b; GAF-AG-BGR, 2009).

In the west, the upper amphibolite to granulite facies rocks of the Ikalamavony Sub-domain consist of a stack of intensely deformed allochthons thrust eastward over the Itremo Sub-domain (Tucker et al., 2007; GAF-AG-BGR, 2009; CGS, 2009a). The Ikalamavony Sub-domain includes a variety of Proterozoic metasedimentary units (Itremo, Ikalamavony and Molo groups) and two suites of intrusive granitoids (Dabolava and Itsindro-Imorona suites; Cox et al., 2004b; Tucker et al., 2007, 2010a,b; CGS, 2009a,b). The Ikalamavony Group comprises mainly metapelites,

metapsammites and metavolcanic rocks. A metarhyolite from the succession has been dated at 1013 ± 10 Ma (CGS, 2009a; Tucker et al., 2010a,b). The Dabolava Suite intrudes the Ikalamavony Group and consists of calc-alkaline gabbroic, tonalitic and granodioritic orthogneisses that have yielded zircon ages between 1013 and 984 Ma (Rakotoarimanana, 2001; Tucker et al., 2007; CGS, 2009a). The eastern part of the Ikalamavony Sub-domain includes an important package of much younger metaclastic rocks (<630 Ma) which Cox et al. (2004a) termed the Molo Group. However, the full extent and distribution of this unit remains unclear (Cox et al., 2004b; GAF-AG-BGR, 2009; CGS, 2009a).

Strongly deformed Imorona-Itsindro Suite orthogneisses are found throughout the sub-domain whereas intercalated slices of Neoarchaean gneisses are much less common (CGS, 2009a). The age of the regional fold-and-thrust deformation is constrained by deformed orthogneisses of latest Neoproterozoic age and the clearly post-tectonic Cambrian granites of the Ambalavao Suite that intrude both sub-domains (Tucker et al., 2007; CGS, 2009a).

3. Post-Archaean, pre-Neoproterozoic cover successions of Madagascar

Three post-Archaean, pre-Neoproterozoic cover successions are recognised in three geographic areas in the northern half of Madagascar (Fig. 3): the Itremo, Sahantaha and Maha groups in western, northern and eastern Madagascar respectively. The following sections give an overview of the lithological and sedimentological character of these groups.

3.1. Itremo Group

3.1.1. Itremo Group in the Itremo Sub-domain

Originally named the "Série Schisto-Quartzo-Calcaire" (SQC) and "Groupe Schisto-Quartzo-Dolomitique", the main outcrops of the Itremo Group occur in the lower grade Itremo Sub-domain ("Massif Schisto-Quartzo-Dolomitique") in the eastern parts of the Itremo-Ikalamavony Domain (Fig. 2, Bésairie, 1964; Moine, 1966, 1974). Here, the well exposed quartzite-marble-pelite package is located in the relatively accessible southern parts of the Central Highlands and represents the best studied group of rocks in Madagascar (Emberger, 1955; Moine, 1968a,b, 1974; Cox et al., 1995, 1996, 1998, 2000, 2001, 2004a,b; Cox and Armstrong, 1997; Raoelison, 1997; Kröner et al., 2000; Fernandez et al., 2001, 2003; Collins et al., 2003a,c; Fernandez and Schreurs, 2003; Inzana et al., 2003; Nédélec et al., 2003; Fitzsimons and Hulscher, 2005; Tucker et al., 2007).

The lower intensity of the deformation and lower grade of metamorphism in the central parts of the Itremo Sub-domain has meant that sedimentary features and stratigraphic relationships are often well preserved. Fernandez et al. (2003) and Fernandez and Schreurs (2003) have measured a minimum thickness of the Itremo Group of at least 2250 m and demonstrate that the succession consists of, from bottom to top, quartzites, lower metapelites, lower metacarbonates and upper metapelites overlain by upper metacarbonates.

The upward-fining quartzites of the central Itremo Sub-domain are medium-grained and moderately- to well-sorted with numerous primary sedimentary structures preserved, such as planar lamination, wave ripples, current ripples and dune cross-bedding (Moine, 1967a,b, 1974; Cox et al., 1998; Fernandez et al., 2003; Fernandez and Schreurs, 2003). Thin metapelitic beds and laterally discontinuous layers of metaconglomerate occur in the upper parts of the metaquartzite units. The generally clast-supported metaconglomerates consist of quartzite cobbles set in a matrix of fine- to
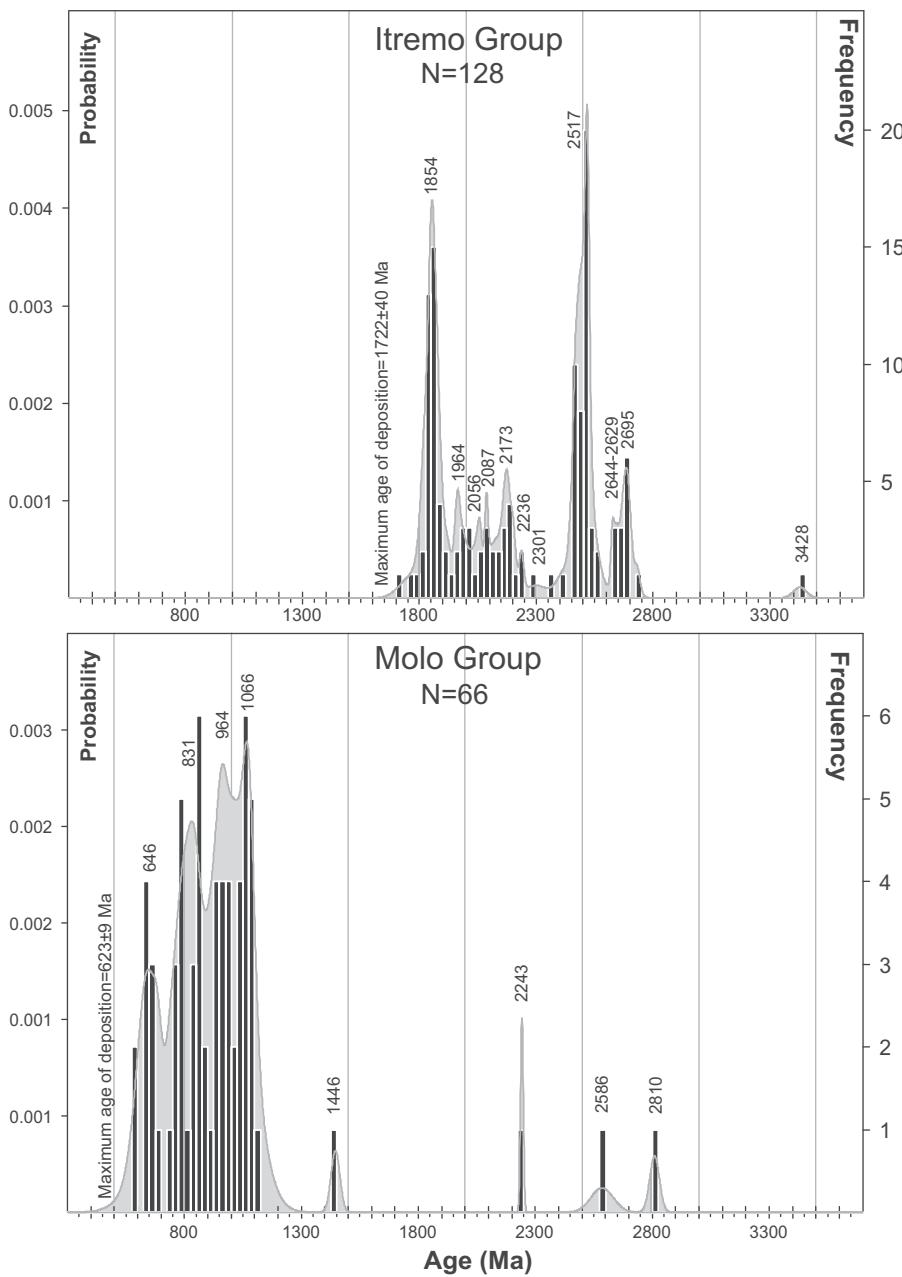
Fig. 4. Relative age-probability curves for the Itremo (top) and Molo Group (bottom). Data after Cox et al. (1998, 2004a) and Fitzsimons and Hulscher (2005).

medium-grained quartz sand (Moine, 1974; Fernandez et al., 2003; Fernandez and Schreurs, 2003; CGS, 2009a). The metapelite layers within the quartzite succession become thicker and more closely spaced upsection, and mark the transition to the overlying pelitic schist unit.

The metapelitic rocks of the central Itremo Sub-domain have traditionally been referred to as "*micaschiste*" by previous workers (Moine, 1968b, 1974) but Cox et al. (1998) preferred to use the general term "pelites" since these rocks consist of laminated siltstones and mudstones metamorphosed at different grades. Fine-grained quartzites with normal grading and asymmetrical hummocky cross-laminations occur as interbeds in the lower metapelite unit, whereas graphite schists occur in the upper metapelite (Fernandez and Schreurs, 2003) (Fig. 4).

The metacarbonates of the central Itremo Sub-domain are dominated by calc-silicates and dolomitic marbles that occur as lower and upper units separated by metapelite in the upper half of the Itremo succession (Fernandez and Schreurs, 2003). Domal and pseudo-columnar stromatolites are relatively common (Fig. 5 in Cox et al., 2004a). The calc-silicates, containing variable amounts of carbonate, quartz and mica, occurring together with metamorphic tremolite and diopside, are found throughout the marbles, but are more common across the transition from metacarbonate to metapelite (Fernandez and Schreurs, 2003). Rare thin amphibolite layers are sometimes observed within the Itremo Group.

In general, most researchers agree that the Itremo Group was deposited on a shallow continental margin, but some differences remain regarding the interpretation of the detailed environmental conditions (Moine, 1967a,b, 1974; Cox et al., 1998; Fernandez et al., 2003; Fernandez and Schreurs, 2003). The most likely age of the Itremo Group is about 1.80–1.65 Ga based on the morphology of stromatolites and the ages of the youngest detrital zircons (Cox and Armstrong, 1997; Cox et al., 1998, 2004a,b; Fernandez et al., 2003).
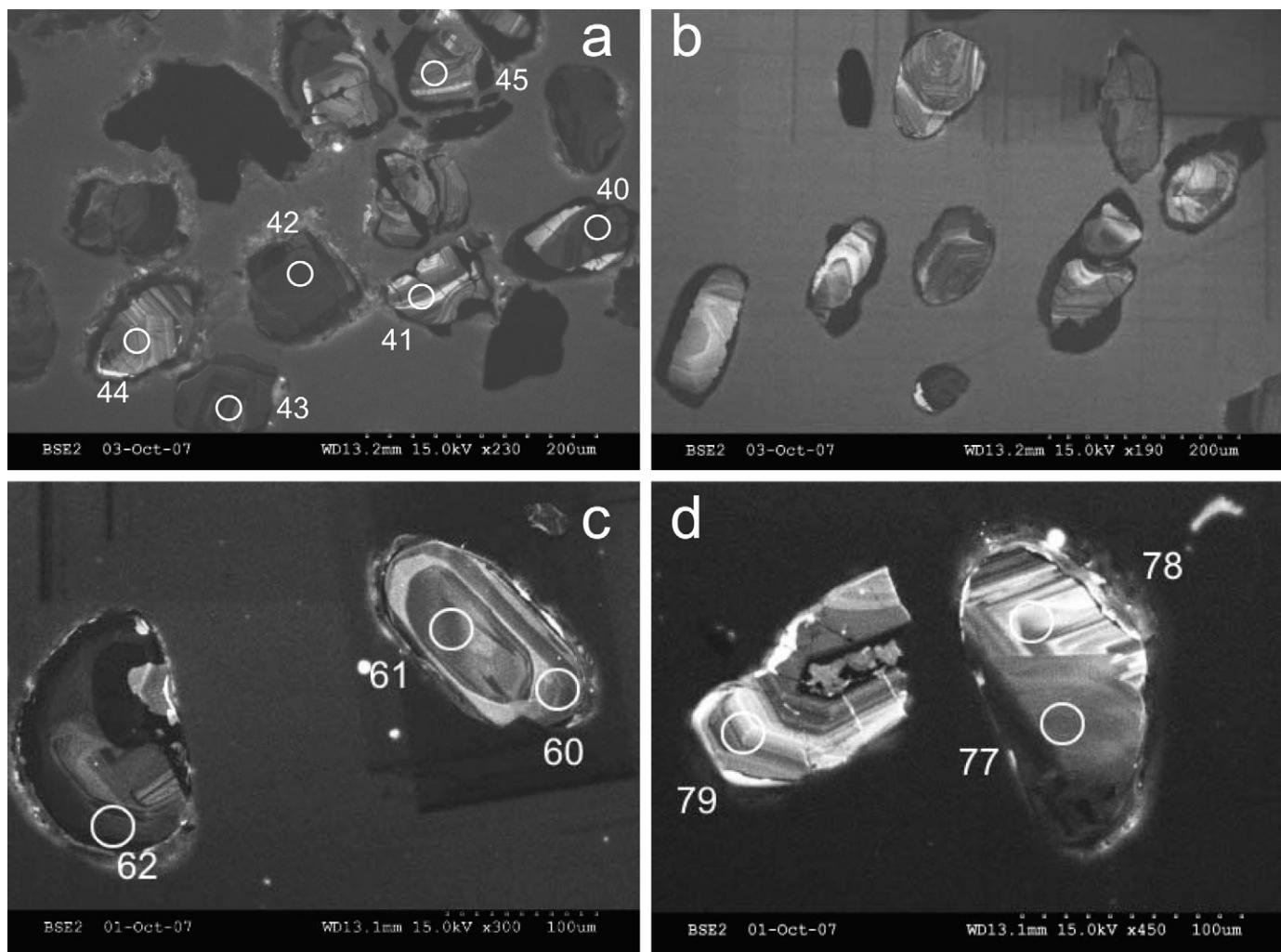
Fig. 5. Cathodo-luminescence imagery of selected zircon grains from samples of the Sahantaha Group; sample RT-06-431 (a, b) and sample BDW197 (c, d).

3.1.2. Itremo Group in the Ikalamavony Sub-domain

Whereas the lithostratigraphy of the Itremo Sub-domain has been relatively well understood since the publication of the 1:200,000 "Groupe Schisto-Quartzo-Dolomitique" (SQD) map of Moine (1968b), the much more intense fold and thrust deformation and the greater lithological and stratigraphic variety has led to a somewhat confusing range of different litho-tectonic subdivisions and stratigraphic nomenclature for the higher grade rocks of the Ikalamavony Sub-domain (Table 1; e.g. Fournié and Heurtebize, 1963; Moine, 1963, 1968b, 1974; Joo, 1963; Alsac, 1963a,b; Bésairie, 1964, 1969; Hottin, 1976; Windley et al., 1994; Tucker et al., 2007; Collins et al., 2000b, 2003a,b,c; Collins, 2006).

The recent CGS (2009a,b) mapping recognised three east-vergent and thrust-bounded mega-lithotectonic packages across the central and northern Ikalamavony Sub-domain (Table 1). The structurally uppermost package includes two main supracrustal rock associations: metapelite-metapsammite-amphibolite-metarhyolite and quartzite-metaconglomerate-marble. The supracrustal rocks are tectonically interleaved with orthogneisses of the Dabolava and Imorona-Itsindro suites and more rarely, thin thrust slices of Antananarivo Craton migmatites. Although these supracrustal rock associations commonly crop out separately, in places the intense infolding and thrusting results in relatively intimate and complex interfingering of the lithodemic units.

The middle lithotectonic package consists of a succession of quartzites and subordinate metaconglomerates up to 2 km thick that form the Bevitsika-Tsinjomay-Kingaly mountains. The lowermost lithotectonic package, which is thrust over the Itremo Sub-domain comprises mostly biotite-quartz-feldspar ± hornblende gneisses tectonically interleaved with thick quartzite-metaconglomerate packages and large volumes of sheared Imorona-Itsindro granite orthogneiss.

Given their lithological similarities to the Itremo Group of the Itremo Sub-domain, the quartzite-metaconglomerate ± marble associations observed in all three packages have been assigned to the Itremo Group (or SQD) by most early mappers (Table 1; Moine, 1963, 1968b; Joo, 1963; Alsac, 1963a,b) and by the CGS (2009a). The metapelite-metapsammite-amphibolite-metarhyolite association in the upper package and the biotite gneisses in the lower package are assigned to the Ikalamavony Group. Dating has revealed an additional, formerly unknown, supracrustal unit in the lower package, the Neoproterozoic Molo Group (Cox et al., 2004a), however the extent of the unit remains largely unknown (Fig. 2).

Moine (1963, 1967a, 1974) considered the Ikalamavony Group rocks to be coeval distal, western facies of the Itremo Group but modern detrital zircon geochronology suggests otherwise. Detrital zircons from the thick quartzite-metaconglomerate Kinangaly-Tsinjomay-Bevitsika mountain ridge in the central Ikalamavony Sub-domain (Fig. 2) yielded Archaean-Palaeoproterozoic age spectra and peak ages similar to those of the Itremo Group in the Itremo Sub-domain (Cox et al., 2004a, see next section) and support their classification as part of the Itremo Group. In contrast, the detrital

Table 1
Tectonic and lithostratigraphic units of the Itremo-Ikalamavony Domain as mapped by the CGS (2009b) with previous subdivisions for comparison.

CGS (2009b)				Bésairie (1964) 1:1 000 000 map	Moine (1968b) 1:200 000 map	Bésairie (1969) 1:500 000 map	Hottin (1976) 1:1 000 000 map	Windley et al., 1994	Collins (et al.) 2003	Collins (et al.) 2006
Litho-tectonic subdivisions		Supracrustal rocks	Orthogneisses						Itremo Sheet	Molo Group
Ikalamavony sub-dop	Upper NW Package Miandrivazo	Ikalamavony Group	Dabolava Suite Imorona-Itsindro Suite	Groupe d'Amborompotsy	–	Migmatite Quartzite Amphibolite	Systeme Amborompotsy-Ikala Serie du Vohimena	Miandrivazo		
	Middle Package Kinangaly-Tinjomay-Bevitsika Ridge	Itremo Group Itremo Group	None	Serie de Schisto Quarzto-Calcaire	–	Serie de Schisto-Quarzto-Calcaire		Serie de Schisto-Quarzto-Calcaire Vohimena		
	Lower SE package Molo	Molo Group	Imorona-Itsindro Suite	Groupe d'Amborompotsy Groupe de Malakialina	Group gneissique	Groupe d' Ikalamavony				
						Ikalamavony Vohimena Malakialina		Vohimena		
Itremo sub-domain		Itremo Group Itremo Group	Imorona-Itsindro Suite	Serie de Schisto-Quarzto-Calcaire/Serie Schisto-Quarzto- Dolomitique						Itremo Group

zircon from the metapelites of the Ikalamavony Group dated by the CGS (2009a) yielded a restricted range of ages between 1070 and 1020 Ma, and a metarhyolite from the unit yielded an extrusion age of 1013 Ma (Tucker et al., 2010b). These new ages clearly demonstrate that the Itremo and Ikalamavony metasedimentary rocks were derived from different sources and cannot be coeval lateral facies equivalents. What remains unresolved is the nature of the original contact relationships between the two, often intimately related units, given that all contacts are now tectonic following the Ediacaran-Cambrian thrusting and folding. Two models are proposed. The first suggests that the Itremo and Ikalamavony were never in sedimentary contact and were only juxtaposed during Ediacaran-Cambrian orogeny. The second model proposes that the Ikalamavony Group was deposited unconformably upon the Itremo Group. Arguments against the unconformity model include: (1) the complete absence of recycled Palaeoproterozoic and older detrital zircons from the Itremo Group in the Ikalamavony Group (CGS, 2009a; Tucker et al., 2010b); (2) unpublished Nd isotope data imply that the Ikalamavony Group metavolcanics are juvenile and show little or no evidence of crustal contamination and (3) field observations suggest the Dabolava Suite intrudes only the Ikalamavony Group suggesting the Itremo and Ikalamavony groups were only juxtaposed during the late Neoproterozoic-Ediacaran Orogeny.

3.1.3. Itremo Group in the Bekodoka Inlier

The Bekodoka Inlier of northwest Madagascar (Fig. 2) has traditionally been subdivided into migmatitic orthogneisses of the Antananarivo Craton and metagreenstones of the Tsaratanana Complex (e.g. Bésairie, 1969) but the recent CGS (2009b) mapping has identified a small, formerly unknown, belt of amphibolite, quartzite and marble in the southwestern parts of the Bekodoka Inlier (Fig. 2). The supracrustal rocks form NW-striking, northeast-vergent tight cylindrical folds that are clearly thrust over older, strongly migmatitic orthogneisses of the Antananarivo Craton along the Kalonja Thrust (KT on Fig. 2, CGS, 2009b). The field appearance, mineralogy and geochemistry of the rock types, the observed rock type associations and the structural and metamorphic characteristics of the belt are strikingly similar to the Itremo and Ikalamavony Group rocks further east in the central Ikalamavony Sub-domain and, along with the new detrital age data presented in this paper, the CGS (2009b) have used these similarities to classify the rocks as the north-westernmost extent of the Itremo-Ikalamavony Domain.

3.2. Sahantaha Group

The rocks we term the Sahantaha Group have been the subject of considerable debate for the pioneering French workers in Madagascar. Based on the mapping by Dormois (1949) and Brenon (1951), the lowermost metasedimentary gneisses of northern Madagascar, lying on Archaean basement, were ascribed to the "*Système de Graphite*", including amphibolite, calc-silicate and quartzite of the "*Série du Sambirano*" of Bésairie (1959). The rocks (quartzites, migmatites and schists, "granitised" at the base) were later called the "*Serie de Sahantaha*" (Bousteyak, 1970, 1972, 1974; Bousteyak et al., 1970-72). Jourde et al. (1978) equated the "Daraina-Milanoa Series" of farther north to the "*Système Supérieure de Andriamena – Sahantaha*". This implied that the Sahantaha and Daraina-Milanoa rocks were possibly lateral equivalents, though this has been shown to be incorrect, in that the Daraina-Milanoa groups are Neoproterozoic in age, and are thus part of the northern Bemarivo Belt (Thomas et al., 2009).

The current phase of mapping has shown that the Sahantaha Group comprises a complex succession of high-grade (upper amphibolite to granulite facies), predominantly metasedimentary gneisses and schists which underlie much of the southern part

of the Bemarivo Belt (Fig. 2). The northern part of the southern Bemarivo Domain is dominated by granitoid orthogneisses of the Antsirabe North Suite, the oldest of which is dated at ca. 758 ± 5 Ma (Thomas et al., 2009). The plutonic rocks locally contain xenoliths of metasedimentary gneisses which are possible correlates of the Sahantaha Group. This is uncertain, but may provide a minimum age for deposition of the group. In the southwest, the Sahantaha Group abuts the high-grade Neoproterozoic Anaboriana-Manampotsy Belt and a short segment of the Antananarivo Craton along the high-angle Sandrakota Shear Zone (SSZ on Fig. 2). In the southeast the rocks are juxtaposed with the Antongil Craton along the Andaparaty thrust (Fig. 2).

The Sahantaha Group has been subdivided into a number of lithodemic units, dominated by high-grade paragneisses and schists. These are locally rhythmically interlayered with thin metapsammite layers ranging up to 1.5 m thick. Quartzites are commonly developed, especially in the south near the craton margins, where they can be up to 300 m thick, and often form marked topographic scarp features at the base of the sequence. Individual quartzite units rapidly pass laterally into enveloping pelitic schists, defining narrow corridors. This relationship is reminiscent of coarse clastic fans or lobes passing out into mud dominated shelf or slope apron deposits and probably reflects the origin of the quartzite as a proximal continental margin sedimentary succession, originally deposited along the northern margin of a craton. In this, units of quartzite are generally gently inclined northwards and overlie the Archaean basement with a low-angled contact, and form a sequence of piggy-backed imbricate structures along a flat-lying basal décollement. In the central parts of the southern Bemarivo Belt, massive to layered pure quartzite units form striking white outcrops where they are well-layered and up to several hundred metres thick.

Calcareous and calcic metasedimentary rocks are a widely distributed and a characteristic feature of the Sahantaha Group, though they are only volumetrically significant in the south, near the margin with the Antongil Craton. In this area massive calc-silicate units crop out, lying structurally above the basal quartzite units.

The only mafic rocks within the Sahantaha Group are layers, pods and lenses of amphibolite. These are quite heterogeneous, ranging from massive to foliated, dark-grey, coarse-grained hornblende-plagioclase rocks to finer-grained laminated biotite amphibolites, often with conspicuous garnet.

3.3. Maha Group

Metasedimentary rocks of the Maha Group overlie the Archaean rocks of the Masora Domain and are overthrust by, and locally tectonically intercalated with, the Neoproterozoic Manampotsy Complex (part of the Anaboriana – Manampotsy Belt) along its western margin (Fig. 2). Intrusive bodies of the 820–760 Ma Imorona-Itsindro Suite are emplaced in, and deformed with, both the Maha Group and Manampotsy Complex.

The Maha Group was first distinguished and described on the Ifanadiana-Mananjary 1:200,000-scale geological map (de la Roche, 1951, 1953). Bertucat et al. (1958) found it impossible to map the Maha and Vohilava groups separately, so a combined Vohilava-Maha series was shown on the 1:100,000-scale geological map of Sheet QR52. The division was reinstated in the 1:500,000-scale compilation map of Bésairie (1970) and is supported by the recent mapping (BGS-USGS-GLW, 2008).

The most extensive outcrop of the Maha Group, the Nosivolo Formation, overlies the northern part of the Masora Craton and can be traced southwestwards into the Maroala Deformation Zone. In the north, the group comprises a medium- to low-grade siliciclastic association of interlayered pelitic and chlorite/talc schists with subordinate feldspathic schists, quartzites and amphibolites. The pelitic schists are characterised by the presence of muscovite, biotite, garnet and/or kyanite.

In the MDZ the Maha Group is represented by garnet-biotite ± kyanite schists and paragneisses with units of locally garnetiferous quartzite, amphibolite and amphibolitised metagabbro, indicating metamorphism at higher pressures within the MDZ than further northeast on the Masora Craton. Thus, metamorphic conditions of 647 °C and 5.6 kb were calculated for the Nosivolo Formation in the north, and temperatures in the range 583–640 °C at a calculated 6.9 kb from a metapelite in the MDZ based on Grt-Bi geothermometer and GASP geobarometry respectively (BGS-USGS-GLW, 2008).

Within the southern half of the Masora Craton, the Maha Group appears to be locally preserved in synforms and thrust slices within the Archaean basement. The relationship with the greenstone association of the Vohilava Group is, however, complex and difficult to resolve. The Maha Group in this sector is typified by the same lithological association as in the north, but appears to be dominated by quartzites and quartzo-feldspathic gneisses with pelitic schist interlayers. Regular repetition of massive-bedded, upward-fining psammitic layers and locally graphitic mica schist are reminiscent of turbiditic sequences. Calcareous rocks are not recorded from the Maha Group, in contrast to the Itremo and Sahantaha groups.

4. Previous detrital age data from the cover sequences

Detrital zircon age data for the cover successions, reported prior to this study, are limited to the Itremo and Molo groups of western Madagascar (Fig. 4, data after Cox et al., 1995, 1996, 1998, 2000, 2001, 2004a,b; Cox and Armstrong, 1997; Fitzsimons and Hulscher, 2005), and a single sample of quartzite in the Sahantaha Group of northern Madagascar (Cox et al., 2003). These studies show that the detrital source of the Itremo Group ranges in age from 3425 to about 1700 Ma (Cox and Armstrong, 1997; Fernandez et al., 2003; Cox et al., 2004a,b). The detrital zircon age patterns are remarkably consistent between samples, with major peaks at approximately 2500 and 1850 Ma and minor peaks at 2700, 2250, 2100 and 2000 Ma (see summary of data in Fitzsimons and Hulscher, 2005). The maximum age of the Itremo Group was constrained by the youngest detrital monazite (1685 ± 29 and 1637 ± 29 Ma; Huber, 2000; Fernandez et al., 2003) and zircon grains (1722 ± 40 Ma; Cox et al., 2004a). The minimum age was constrained by the ca. 800 Ma Imorona–Itsindro Suite orthogneisses that intrude the group (Handke et al., 1999; Kröner et al., 1999a,b; Tucker et al., 2007). A similar succession from the Molo Group yielded a youngest detrital zircon age of around 623 Ma, and was interpreted as having been deposited between that time and around 523 Ma, the age of metamorphic rims (Cox et al., 2004a). Cox et al. (2003) also reported limited data on the Sahantaha Group, which showed detrital zircon ages concentrated at 1834 ± 4 Ma and 2502 ± 8 Ma, suggesting some similarity to the detrital patterns of the Itremo Group.

Although the contacts are strongly tectonised, it has been suggested that the Itremo Group was deposited unconformably onto the Archaean migmatitic gneisses of the Antananarivo Craton of central Madagascar (Cox et al., 1998). Evidence for this includes (1) the observation that the detrital zircons from the Itremo Group show age peaks at ca. 2700, 2500 and 2450 Ma (major peaks), broadly equivalent to the main inheritance, crystallisation and migmatisation ages collected from the migmatitic gneisses of the Antananarivo Craton (Kröner et al., 1999a,b, 2000; Kröner, 2001; Fernandez et al., 2003; Fernandez and Schreurs, 2003; Cox et al., 2004a; Tucker et al., 2007; CGS, 2009b); and (2) field evidence showing that localised metaconglomerate units are proximal to, and in a few cases directly overlie basement gneisses (Cox et al.,

Table 2
Characteristics of zircon analysed from the samples in this study.

Sample	Colour	Size (urn)	Aspect ratio	Morphology	Internal zoning	Interpretation
RT-06-431	Colourless, clear	50–200	1:1–2:1	Subhedral to euhedral, pitted surfaces and rounding	Concentric zoning, some have a narrow dark-CL rim	Detrital grains from dominant magmatic sources
BDW197	Colourless, clear	50–150	1:1–2:1	Subhedral to euhedral, pitted surfaces and rounding	Concentric zoning, some have a narrow dark-CL rim	Detrital grains from dominant magmatic sources
CP183b	Colourless, clear	50–200	1:1–3:1	Subhedral to euhedral, pitted surfaces and variable rounding	Concentric zoning, some complex grains with core and rim domains. Rims are narrow and dark-CL	Detrital grains from dominant magmatic sources
PP727	Colourless, clear	50–200	1:1–3:1	Subhedral to euhedral, pitted surfaces and rounding	Concentric zoning, some complex grains with core and rim domains. Rims are narrow and dark-CL	Detrital grains from dominant magmatic sources
PF06035	Colourless, to dark brown	50–250	1:1–3:1	Subhedral, pitted surfaces and rounding	Concentric and broad zoning. Some broad and dark-CL rims	Detrital grains from dominant magmatic sources
PR06088	Colourless, brown, mainly slightly turbid	100–200	1:1–2:1	Subhedral to anhedral, pitted surfaces and rounding	Concentric zoning, some have a narrow dark-CL rim	Detrital grains from dominant magmatic sources

1998). Both the Itremo Group and the Antananarivo basement are intruded by mid-Neoproterozoic (ca. 800 Ma) orthogneisses of the Imorona-Itsindro Suite (Handke et al., 1999; Tucker et al., 1999, 2007; Kröner et al., 2000) indicating that the unconformity must predate these intrusions. The detrital zircon provenance analysis of the Itremo Group completed by Cox et al. (2004a) recognised several zircon age peaks that indicate that the Itremo Group was derived from local sources (Antananarivo Craton) and rocks in East Africa, and that the Antananarivo Craton might therefore have been adjacent to the Congo/Tanzania/Bangweulu Block in the Late Palaeoproterozoic/Early Mesoproterozoic. They also concluded that the detrital zircon and sedimentological similarities between rocks of the Itremo Group and the Zambian Muva Supergroup suggest a possible lithostratigraphic correlation between the two (Cox et al., 2004a).

4.1. New Detrital zircon U–Pb geochronology

Two samples from each of the Sahantaha, Maha and Itremo Groups were processed to separate detrital zircons for provenance analysis. Samples from the former two groups were analysed by laser ablation multi-collector-ICP-MS (LA-MC-ICP-MS) at the NERC Isotope Geosciences Laboratory, British Geological Survey, UK, whilst the samples from the Itremo Group were analysed using sensitive high resolution ion microprobe (SHRIMP) at the Research School of Earth Sciences, Australian National University, Canberra, Australia. Full details of the techniques and validation results are available in the methodology section in the online repository. Final data were plotted and data point ages determined using Isoplot (Ludwig, 2003) with statistics and combined probability density distributions (PDDs) and histograms produced using the 'Age Display' macro of Sircombe (2004) for Microsoft Excel. Histogram bin widths were selected to reflect the total uncertainty distribution of the data points and to maximise the histogram efficiency whilst providing the best coincidence of histogram and PDD peak profiles.

4.2. Sahantaha Group

Detrital zircons from two samples of Sahantaha quartzite were analysed by LA-MC-ICP-MS. Sample RT-06-431 (see sample position Fig. 3) was collected from an outcrop of clean, medium- to coarse-grained, bedded quartzite.103 analyses were conducted on zircon domains that show prominent concentric internal zoning patterns (Tables 2 and 3, Fig. 5a and b). Of these, 42 analyses plot $100 \pm 5\%$ concordant, with remaining analyses defining crude arrays below the concordia line on a Wetherill plot (see Fig. 6a and Table 3), indicating variable amounts of non-zero Pb-loss. Assessment of $^{207}Pb/^{206}Pb$ data within 5% of concordance indicates a mean uncertainty of the data point ages of 14.6 Ma (2σ) and a

histogram bin width efficiency of 81.4% (at 30 Ma bin width). Considering this mean age uncertainty and rounding to the nearest 10 Ma, the probability density distribution indicates age maxima at: 3190, 3170, 2880, 2690, 2440, 2290, 2240, 2080, 1910, 1860, 1850, 1830 and 1800 Ma. Maxima within uncertainty define age ranges of 3190–3170 and 1860–1800 Ma (see Fig. 6b), of which the latter is by far the largest grouping with 32 of the 42 concordant data points. The youngest concordant zircon in this dominant population has a $^{207}Pb/^{206}Pb$ age of 1771 ± 18 Ma (2σ), which is interpreted as the maximum age of deposition of the quartzite.

Sample BDW197 (see sample position on Fig. 3) was collected from a large outcrop of sillimanite-bearing quartzite in the Sahantaha Group. The zircon grains show very similar morphologies and internal zoning patterns to those from sample RT-06-431, with variable sedimentary rounding and internal concentric zoning (Table 2, Fig. 5c and d). 49 analyses plot on or within $100 \pm 5\%$ of concordia, whilst the remainder plot variably discordant along non-zero Pb-loss trends (Table 4, Fig. 6c). Assessment of $^{207}Pb/^{206}Pb$ ages of concordant (>95%) data indicates a mean uncertainty of the data point ages of 18.2 Ma (2σ) and a histogram bin width efficiency of 83.3% (at 40 Ma bin width). The probability density distribution indicates age maxima at: 2620, 2500, 2470, 2310, 2260, 2240, 2180, 2100, 2070, 2040, 1921, 1820 and 1760 Ma (Fig. 6d) rounded to the nearest 10 Ma. Maxima within uncertainty define age ranges of 2500–2470, 2260–2240 and 2100–2040 Ma. By far the largest mode is that at 1820 Ma which comprises 22 of the 49 concordant data points. The youngest detrital zircon with an age of 1745 ± 18 Ma provides the maximum age of deposition for this quartzite of the Sahantaha Group, agreeing within uncertainty with that for sample RT-06-431.

4.3. Maha Group

Two samples were analysed from the Maha Group on the Masora Domain. Sample CP183b was collected from a quartzite that forms part of a succession of quartzite, metapelite and minor metaconglomerate. 82 analyses were conducted by LA-MC-ICP-MS on both single sector zircon and core-rim domains of complex zircon grains (Tables 2 and 5, Fig. 7a and b). The data range from concordant to strongly discordant, with 47 analyses plotting within 5% of concordia (Table 5, Fig. 8a). U content is in the range 53–1337 ppm, with the highest contents recorded in sectors interpreted as an igneous phase. Analyses on high uranium overgrowths have U contents of between 221 and 951 ppm, but inspection of CL imagery shows that due to the relatively small size of these zones ($\sim$20 μm) the laser spot in all but one case (analysis 77, see Fig. 7a) possibly intersects both core and rim phases, lending some doubt to the interpretation of these analyses. Assessment of "concordant" (>95%) data indicates a mean

Table 3
Zircon U–Pb LA-MC-ICP-MS data for sample RT-06-431.

Spot	^{204}Pb (cps)	^{206}Pb (mV)	^{238}U (mV)	Pb (ppm)	U (ppm)	^{238}U/^{206}pb	ls%	^{207}pb/^{206}pb	ls%	^{207}pb/^{206}pb	2s abs	^{206}Pb/^{238}U	2s abs	%C
15	–	7	20	96	219	2.279	1.9	0.2046	0.50	2864	16	2345	74	82
16	–	12	32	166	349	2.065	1.9	0.2005	0.50	2830	16	2546	80	90
17	445	11	48	153	528	3.295	3.0	0.1546	1.17	2398	40	1709	90	71
18	–	8	45	105	492	4.302	4.2	0.1014	1.49	1650	55	1347	102	82
19	–	4	30	60	331	4.895	4.6	0.0928	1.43	1484	54	1198	99	81
20	–	8	38	116	413	3.520	2.2	0.1087	0.50	1777	18	1612	63	91
21	–	4	13	61	148	2.388	2.0	0.1448	0.50	2285	17	2255	76	99
22	–	5	20	68	219	3.187	2.0	0.1099	0.50	1798	18	1759	62	98
23	–	8	46	118	503	4.183	2.0	0.1042	0.50	1701	18	1382	51	81
24	–	3	12	43	128	2.948	1.9	0.1122	0.50	1836	18	1883	62	103
25	–	12	97	168	1062	6.121	2.9	0.0936	1.07	1500	41	975	53	65
26	–	3	11	48	118	2.391	1.9	0.1407	0.50	2236	17	2252	71	101
27	–	4	14	57	152	2.582	1.9	0.1286	0.50	2078	18	2110	69	102
28	–	8	68	116	744	6.209	2.0	0.0970	0.50	1566	19	963	36	61
29	–	10	72	134	786	5.727	2.0	0.0956	0.50	1540	19	1037	37	67
30	–	7	30	104	325	3.032	2.0	0.1130	0.50	1848	18	1838	64	99
31	–	2	10	33	105	3.050	2.0	0.1125	0.50	1840	18	1828	62	99
32	–	4	16	56	176	3.069	2.0	0.1128	0.50	1845	18	1818	63	99
33	–	6	36	91	390	4.158	2.0	0.1048	0.50	1711	18	1389	51	81
34	–	4	16	54	172	3.116	1.9	0.1141	0.50	1866	18	1794	59	96
35	–	11	42	148	458	3.037	1.9	0.1117	0.50	1827	18	1835	61	100
36	–	5	30	71	327	4.003	4.4	0.1024	1.39	1668	51	1438	113	86
37	–	5	21	74	235	3.061	1.9	0.1111	0.50	1818	18	1822	59	100
38	–	6	25	90	279	3.001	2.0	0.1121	0.50	1834	18	1854	63	101
39	–	11	46	148	510	3.358	1.9	0.1097	0.50	1794	18	1680	57	94
40	–	9	46	110	482	3.922	1.3	0.1141	0.50	1865	18	1464	33	79
41	664	6	39	68	403	5.118	2.8	0.1132	0.58	1852	21	1151	60	62
42	–	11	47	132	494	3.328	1.0	0.1111	0.50	1818	18	1694	31	93
43	373	16	57	195	598	2.735	1.1	0.2392	0.50	3114	16	2009	39	65
44	–	4	14	47	144	2.691	1.4	0.1505	0.50	2352	17	2037	48	87
46	–	8	31	92	325	3.077	1.3	0.1109	0.50	1815	18	1814	40	100
47	–	6	24	75	251	2.978	1.6	0.1627	0.50	2484	17	1867	50	75
48	–	7	29	79	303	3.241	1.7	0.1098	0.50	1797	18	1734	51	96
49	–	7	39	82	402	4.158	3.1	0.1069	0.51	1746	19	1389	76	80
50	–	14	56	165	588	3.160	1.1	0.1102	0.50	1802	18	1772	33	98
51		3	15	41	156	3.388	1.2	0.1313	0.50	2116	18	1667	34	79
52		7	29	88	302	3.045	1.1	0.1111	0.50	1817	18	1830	35	101
53	–	8	32	92	332	3.205	1.1	0.1099	0.50	1797	18	1751	33	97
54	–	8	50	92	525	4.225	3.9	0.1313	2.36	2116	83	1369	96	65
56	–	6	27	76	282	3.257	1.1	0.1105	0.50	1808	18	1726	32	95
57	–	2	9	28	93	2.868	1.1	0.1170	0.50	1911	18	1928	38	101
58	–	7	20	83	209	2.227	1.2	0.1584	0.50	2439	17	2391	47	98
59	–	2	7	21	74	3.076	1.1	0.1098	0.58	1796	21	1815	36	101
60	–	8	40	102	422	3.657	3.3	0.1058	0.83	1728	31	1558	92	90
61	–	3	14	42	150	3.183	1.1	0.1112	0.50	1819	18	1761	33	97
62	–	5	17	54	179	2.928	1.3	0.1125	0.50	1840	18	1894	42	103
63	358	8	50	102	517	4.363	1.9	0.1104	1.10	1806	40	1330	46	74
64	–	5	22	62	225	3.190	1.2	0.1116	0.50	1826	18	1758	35	96
65	–	7	48	84	500	4.971	3.6	0.0961	1.37	1550	51	1181	77	76
66	–	11	84	131	873	5.659	2.5	0.0955	1.16	1538	44	1049	48	68
67	–	11	47	136	489	3.153	1.3	0.1100	0.50	1800	18	1776	39	99
68	–	7	31	82	320	3.372	1.1	0.1083	0.50	1771	18	1674	32	95
69	–	9	62	106	650	4.716	5.7	0.0960	2.61	1547	98	1240	128	80
70	–	7	32	79	332	3.715	2.2	0.1091	0.50	1785	18	1537	59	86
71	–	9	42	111	439	3.515	1.1	0.1152	0.52	1882	19	1614	33	86
72	–	12	44	148	463	2.781	1.3	0.1418	0.50	2249	17	1980	45	88
73	–	12	126	149	1314	7.865	1.1	0.0856	0.71	1329	28	111	17	58
74	–	7	36	78	372	4.244	1.6	0.1039	0.50	1695	18	1364	40	80
75	–	2	13	22	132	4.065	5.8	0.0989	3.09	1603	115	1418	145	88
76	–	11	46	137	482	3.115	1.1	0.1104	0.50	1806	18	1795	34	99
77	–	6	27	76	283	3.331	1.3	0.1096	0.50	1792	18	1692	37	94
78	–	11	74	129	773	5.359	1.3	0.0965	0.50	1557	19	1103	27	71
79	–	7	32	80	334	3.688	1.2	0.1061	0.50	1734	18	1547	32	89
80	–	7	40	85	414	4.108	3.7	0.1068	0.85	1745	31	1405	92	80
81	–	3	8	36	79	1.920	1.1	0.1835	0.50	2685	17	2702	49	101
A	–	7	14	95	334	3.433	1.5	0.1133	0.50	1854	8	1648	43	89
B	–	9	9	116	216	1.825	1.0	0.2068	0.50	2881	4	2817	46	98
C	–	6	10	74	229	2.909	1.0	0.1121	0.50	1834	8	1905	34	104
D	–	4	8	56	180	2.956	1.6	0.1140	0.50	1864	11	1878	51	101
F	–	12	11	151	255	1.636	2.0	0.2479	0.50	3171	3	3076	97	97
G	–	4	7	56	173	2.958	2.1	0.1127	0.50	1843	11	1877	67	102
H	–	8	13	101	306	2.917	1.5	0.1117	0.50	1827	7	1900	48	104
1	–	9	18	119	427	3.434	1.1	0.1098	0.50	1796	6	1648	33	92
J	–	5	8	58	197	3.315	1.1	0.1107	0.50	1810	11	1699	34	94
K	–	7	13	96	296	2.969	1.9	0.1143	0.50	1869	7	1871	61	100
L	–	4	8	58	182	2.896	1.3	0.1616	0.50	2473	7	1912	42	77

Table 3 (*Continued*)

Spot	^{204}Pb (cps)	^{206}Pb (mV)	^{238}U (mV)	Pb (ppm)	U (ppm)	^{238}U/^{206}pb	ls%	^{207}pb/^{206}pb	ls%	^{207}pb/^{206}pb	2s abs	^{206}Pb/^{238}U	2s abs	%C
M	–	12	28	156	643	3.821	1.1	0.1083	0.50	1771	5	1499	30	85
N	–	7	24	92	568	5.794	1.6	0.0943	0.64	1515	24	1026	30	68
0	–	4	10	49	232	4.492	1.5	0.1194	0.53	1947	19	1296	35	67
P	–	7	11	96	265	2.628	1.1	0.1474	0.50	2316	7	2079	40	90
Q	–	14	33	184	763	3.960	1.1	0.1074	0.50	1756	4	1452	29	83
R	–	2	7	31	166	4.972	1.5	0.1116	1.25	1826	45	1181	32	65
S	–	9	20	122	458	3.455	0.9	0.1120	0.50	1833	6	1639	27	89
T	–	2	3	20	61	2.880	1.0	0.1173	0.68	1915	24	1921	33	100
U	–	15	98	196	2278	10.767	1.2	0.0606	0.50	627	18	573	13	91
V	–	6	12	76	270	3.197	1.6	0.1121	0.50	1834	8	1754	50	96
w	–	9	17	119	401	3.120	1.0	0.1131	0.50	1849	6	1792	33	97
X	–	6	11	77	262	3.088	1.0	0.1133	0.50	1853	8	1808	32	98
Y	–	5	9	65	220	3.060	1.1	0.1128	0.50	1845	10	1823	34	99
AA	–	7	13	90	307	3.050	1.8	0.1139	0.50	1862	7	1828	56	98
AB	–	4	32	54	750	12.481	1.4	0.0699	0.50	925	18	497	14	54
AC	–	2	5	30	117	3.521	2.2	0.1375	0.50	2196	14	1612	61	73
AF	–	6	9	76	214	2.651	1.1	0.1361	0.50	2178	7	2063	40	95
AG	–	7	21	97	478	4.520	1.9	0.0999	0.50	1622	9	1288	45	79
AH	–	3	25	44	588	12.272	1.6	0.0744	0.51	1051	21	505	16	48
Al	–	7	7	95	156	1.520	2.0	0.2502	0.50	3186	5	3258	102	102
AJ	–	10	23	127	537	3.844	1.7	0.1097	0.50	1795	6	1491	45	83
AK	–	8	15	108	349	2.927	1.6	0.1130	0.50	1848	6	1894	52	103
AL	–	7	13	87	312	3.355	2.0	0.1132	0.50	1851	8	1682	60	91
AM	–	15	33	189	761	3.615	1.1	0.1499	0.50	2345	4	1574	31	67
AP	–	6	26	79	604	7.066	4.7	0.1458	1.93	2298	66	853	74	37
AN	–	9	31	122	714	5.205	1.3	0.1021	0.50	1663	7	1133	27	68
AO	–	4	8	53	179	3.043	2.7	0.1304	0.50	2103	13	1832	85	87
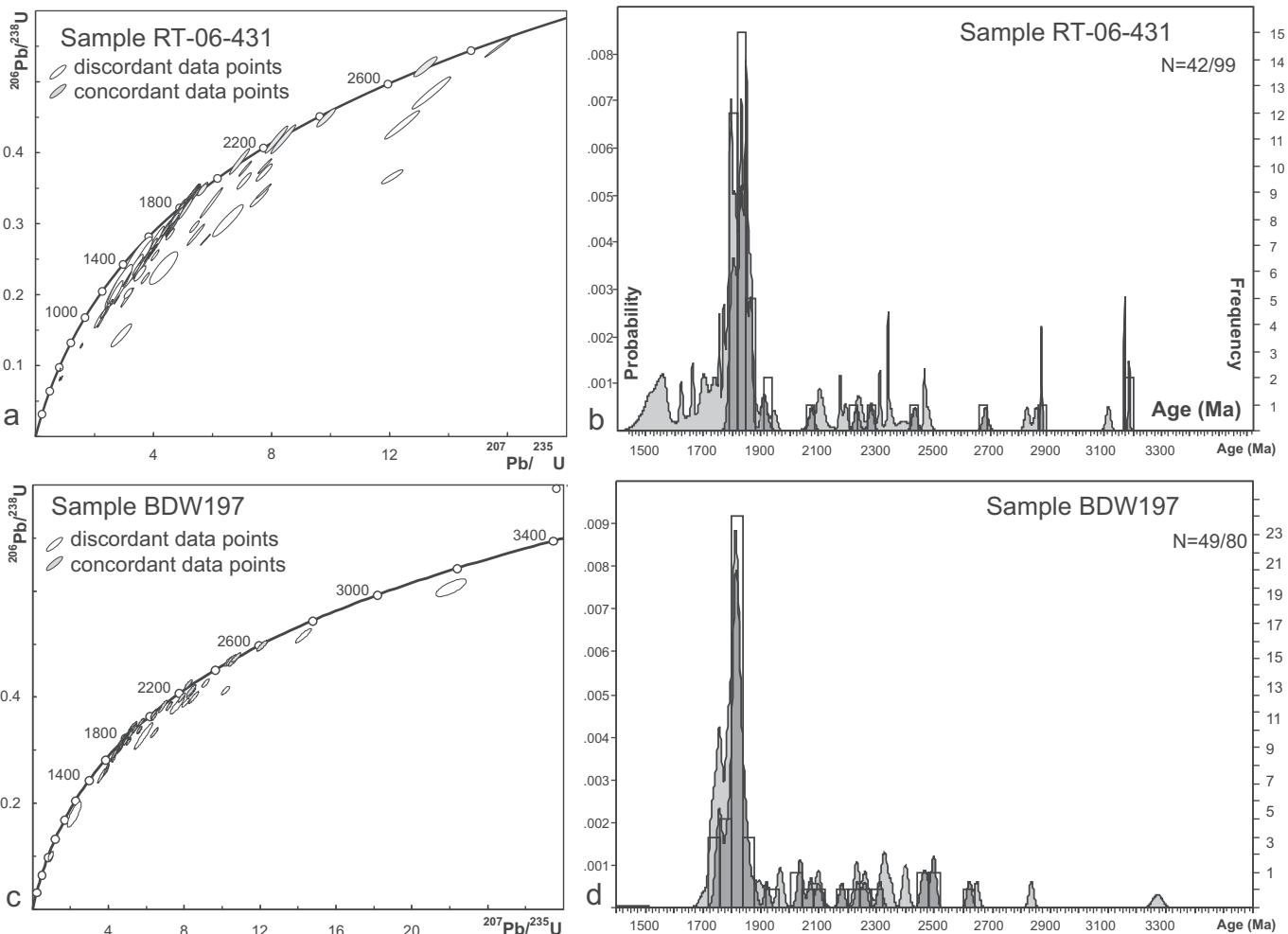
Fig. 6. Plots for LA-MC-ICP-MS zircon U–Pb data for samples from the Sahantaha Group; (a) and (b) Wetherill plot and combined probability-density/histogram plot for sample RT-06-431; (c) and (d) Wetherill plot and combined probability-density/histogram plot for sample BDW197. Uncertainty ellipses are shown at 2σ confidence level. Histogram bin-size is 30 million years for RT-06-431 and 40 million years for BDW197 (only 100 ± 5% concordant data are shown in the histogram).

Table 4
Zircon U–Pb LA-MC-ICP-MS data for sample BDW197.

Spot	^{204}Pb (cps)	^{206}Pb (mV)	^{238}U (mV)	Pb (ppm)	U (ppm)	^{238}U/^{206}pb	1s%	^{207}pb/^{206}pb	1s%	^{207}pb/^{206}pb	2s abs	^{206}Pb/^{238}U	2s abs	%C
2	–	14	52	196	613	3.360	1.1	0.1094	0.50	1789	18	1680	31	94
3	–	16	35	225	413	1.944	1.1	0.2011	0.50	2835	16	2675	48	94
6	–	12	40	174	469	3.034	1.3	0.1400	0.50	2227	17	1837	40	82
7	–	10	35	136	413	3.274	1.1	0.1073	0.50	1755	18	1718	32	98
9	–	7	20	93	237	2.636	1.3	0.1301	0.50	2100	18	2073	46	99
10	–	8	28	110	335	3.216	1.1	0.1078	0.50	1763	18	1745	32	99
1rep	–	7	26	104	314	2.957	0.9	0.1104	0.50	1807	18	1878	28	104
5rep	–	8	27	107	324	2.970	0.9	0.1148	0.50	1877	18	1871	28	100
11	–	6	23	90	271	2.993	0.9	0.1104	0.50	1806	18	1858	29	103
12	–	6	28	85	332	3.865	1.5	0.1073	0.50	1754	18	1483	40	85
13	–	25	94	354	1121	3.140	1.5	0.1091	0.50	1784	18	1782	46	100
14	–	9	36	120	423	3.458	1.7	0.1062	0.50	1734	18	1637	49	94
16	–	17	74	245	875	3.530	1.2	0.1061	0.50	1733	18	1608	33	93
17	–	4	14	52	167	3.096	3.2	0.1300	0.96	2098	34	1804	99	86
18	–	12	48	169	564	3.252	1.0	0.1075	0.50	1758	18	1729	29	98
19	–	8	32	116	381	3.222	0.8	0.1067	0.50	1745	18	1742	24	100
20	–	16	48	225	567	2.439	1.1	0.1471	0.50	2312	17	2215	42	96
21	–	9	35	131	421	3.125	0.9	0.1075	0.50	1758	18	1790	28	102
22	–	10	42	218	701	3.198	0.9	0.1161	0.50	1897	18	1754	28	92
23	–	8	31	184	519	2.779	0.8	0.1281	0.50	2071	18	1982	26	96
24	–	4	16	85	269	3.102	0.8	0.1109	0.50	1814	18	1801	25	99
25	–	7	29	153	486	3.128	0.8	0.1107	0.50	1810	18	1788	25	99
26	–	7	24	158	404	2.521	1.2	0.1543	0.50	2395	17	2154	43	90
27	–	35	141	755	2360	3.107	0.9	0.1112	0.50	1819	18	1799	27	99
28	–	14	57	298	945	3.112	0.8	0.1107	0.50	1811	18	1796	25	99
29	–	16	78	342	1309	3.763	0.8	0.1062	0.50	1735	18	1519	22	88
30	–	5	21	109	349	3.182	0.9	0.1102	0.50	1803	18	1762	27	98
31	–	3	15	76	251	3.261	1.0	0.1093	0.50	1788	18	1724	29	96
31 B	–	5	19	100	323	3.157	0.8	0.1098	0.50	1796	18	1774	24	99
32	–	5	19	102	310	2.976	0.8	0.1111	0.50	1817	18	1867	26	103
33	–	9	25	186	410	2.147	0.9	0.1603	0.50	2459	17	2465	35	100
34	–	6	30	140	494	3.460	0.9	0.1071	0.50	1750	18	1637	27	94
35	–	5	12	117	199	1.651	1.1	0.2641	1.03	3272	32	3053	55	93
36	–	4	13	82	211	2.484	0.8	0.1484	0.50	2327	17	2181	30	94
37	–	4	11	84	182	2.150	0.8	0.1640	0.50	2497	17	2462	33	99
38	–	26	88	560	1467	2.586	0.9	0.1503	0.50	2349	17	2107	33	90
39	–	5	14	101	241	2.369	0.8	0.1406	0.50	2234	17	2270	32	102
40	–	21	73	457	1221	2.617	1.8	0.1436	0.91	2271	31	2086	64	92
41	–	6	25	125	416	3.297	0.9	0.1089	0.50	1780	18	1708	27	96
42	–	7	29	156	479	2.991	0.9	0.1105	0.50	1807	18	1859	30	103
43	–	3	10	58	168	2.855	0.8	0.1177	0.50	1921	18	1936	26	101
44	–	14	45	313	749	2.360	0.8	0.1553	0.50	2405	17	2277	29	95
45	–	3	10	62	174	2.733	0.8	0.1254	0.50	2034	18	2010	27	99
46	328	4	18	97	301	3.051	0.8	0.1105	0.50	1808	18	1827	25	101
47	–	5	23	112	382	3.336	0.9	0.1091	0.50	1784	18	1690	27	95
48	–	5	25	119	415	3.466	0.9	0.1080	0.50	1765	18	1634	26	93
49	–	5	20	101	339	3.336	0.8	0.1094	0.50	1790	18	1690	24	94
50	–	3	24	67	400	5.742	5.8	0.0887	4.08	1398	156	1035	110	74
51	–	8	34	185	569	3.021	0.8	0.1111	0.50	1817	18	1844	26	101
50 B	–	5	24	100	404	4.043	2.3	0.1044	0.78	1703	29	1425	58	84
50 A	–	2	28	44	465	10.556	3.7	0.0686	4.74	886	196	583	41	66
52	–	7	18	149	305	2.019	0.8	0.1766	0.50	2621	17	2594	35	99
53	–	4	12	78	193	2.438	0.8	0.1793	0.50	2646	17	2216	29	84
54	–	4	14	76	237	3.075	0.8	0.1133	0.50	1853	18	1815	25	98
55	–	9	46	196	766	3.876	0.9	0.1077	0.50	1762	18	1480	23	84
56	–	4	18	81	292	3.577	0.8	0.1090	0.50	1783	18	1589	24	89
57	–	6	22	132	367	2.739	1.0	0.1257	0.50	2038	18	2007	34	98
58	–	10	28	214	464	2.137	0.9	0.1616	0.50	2473	17	2475	36	100
59	–	10	39	207	659	3.150	0.9	0.1114	0.50	1822	18	1777	29	98
60	–	7	28	153	461	2.991	0.8	0.1203	0.50	1961	18	1859	26	95
61	–	5	18	102	306	2.987	0.9	0.1211	0.50	1972	18	1862	28	94
62	–	9	31	203	515	2.519	0.9	0.1426	0.50	2259	17	2155	34	95
63	–	7	29	150	477	3.144	0.9	0.1113	0.50	1821	18	1780	27	98
64	–	9	36	187	600	3.136	1.3	0.1107	0.50	1811	18	1784	41	99
65	–	3	11	60	185	3.055	0.8	0.1117	0.50	1827	18	1825	26	100
66	–	21	81	456	1349	2.900	0.8	0.1119	0.50	1831	18	1910	28	104
67	–	6	17	133	284	2.113	0.8	0.1641	0.50	2498	17	2498	34	100
68	–	6	26	132	437	3.316	1.1	0.1104	0.50	1806	18	1699	32	94
69	–	2	9	52	156	2.992	0.8	0.1120	0.50	1832	18	1859	25	101
70	–	1	5	28	81	2.924	0.8	0.1120	0.82	1831	30	1897	26	104
71	–	11	40	249	660	2.631	0.9	0.1363	0.50	2181	17	2077	32	95
72	–	19	61	413	1024	2.455	0.8	0.1486	0.50	2330	17	2203	30	95
73	–	15	59	329	986	2.964	0.8	0.1122	0.50	1836	18	1874	26	102
74	–	7	29	142	477	3.337	0.9	0.1106	0.50	1809	18	1689	25	93
75	–	4	19	97	313	3.200	0.9	0.1111	0.50	1817	18	1753	26	96
76	–	2	8	46	138	2.948	0.9	0.1131	0.52	1850	19	1883	28	102
77	–	5	21	109	346	3.195	0.8	0.1114	0.50	1823	18	1755	24	96
78	–	2	7	37	115	3.048	0.9	0.1134	0.61	1854	22	1829	29	99
79	–	3	11	57	182	3.200	0.8	0.1123	0.50	1838	18	1753	26	95
80	–	8	43	175	719	4.057	0.9	0.1057	0.50	1726	18	1420	22	82

Table 5
Zircon U–Pb LA-MC-ICP-MS data for sample CP183b.

| Spot	^{204}Pb (cps)	^{206}Pb (mV)	^{238}U (mV)	Pb (ppm)	U (ppm)	^{238}U/^{206}pb	1s%	^{207}pb/^{206}pb	1s%	^{207}pb/^{206}pb	2s abs	^{206}Pb/^{238}U	2s abs	%C
2	310	6	23	99	289	2.991	1.2	0.1149	0.50	1878	18	1860	37	99
3	–	1	6	24	71	3.078	1.2	0.1143	0.73	1869	26	1814	37	97
4	–	21	90	349	1118	3.260	1.1	0.1145	0.50	1872	18	1725	34	92
5	–	6	24	101	299	3.008	1.2	0.1148	0.50	1876	18	1850	38	99
6	–	6	23	102	288	2.848	1.3	0.1300	0.50	2098	18	1940	42	92
7	332	9	36	155	448	2.904	1.1	0.1295	0.50	2091	18	1908	38	91
8	533	7	42	123	523	4.329	1.3	0.1434	0.50	2268	17	1340	31	59
9	386	4	22	75	271	3.625	1.2	0.1108	0.50	1813	18	1571	33	87
10	440	6	19	105	238	2.282	1.2	0.1627	0.50	2484	17	2343	47	94
11	486	4	17	70	210	3.015	1.2	0.1131	0.50	1850	18	1847	37	100
12	422	2	10	40	121	3.028	1.2	0.1126	0.50	1841	18	1840	38	100
13	526	22	71	374	885	2.379	1.2	0.1732	0.50	2589	17	2262	45	87
14	674	7	27	116	335	2.915	1.4	0.1512	0.50	2360	17	1901	44	81
16	–	8	39	142	484	3.426	1.1	0.1157	0.50	1890	18	1651	33	87
18	–	9	27	150	331	2.175	1.2	0.1623	0.50	2480	17	2438	49	98
19	–	6	24	96	297	3.082	1.1	0.1141	0.50	1866	18	1811	35	97
20	–	2	10	40	123	3.065	1.2	0.1134	0.50	1855	18	1821	38	98
21	–	3	14	47	177	3.702	1.1	0.1124	0.50	1839	18	1541	31	84
22	–	10	27	162	334	2.038	1.2	0.1781	0.50	2635	17	2574	52	98
23	–	9	40	146	495	3.397	1.3	0.1109	0.50	1814	18	1663	37	92
24	–	4	17	70	216	3.035	1.2	0.1224	1.41	1992	50	1836	38	92
25	–	12	47	196	593	3.055	1.2	0.1252	0.50	2032	18	1825	37	90
26B	–	2	5	29	67	2.311	1.2	0.1533	0.50	2383	17	2318	48	97
27	–	15	66	252	823	3.235	1.2	0.1163	0.50	1900	18	1736	37	91
28	–	13	40	226	501	2.195	1.3	0.1626	0.50	2483	17	2420	51	97
29	–	7	24	113	297	2.584	1.2	0.1430	0.50	2264	17	2109	43	93
30	–	14	61	242	758	3.081	1.2	0.1131	0.50	1850	18	1812	37	98
31	–	5	19	77	234	2.997	1.2	0.1152	0.50	1882	18	1856	37	99
32	–	5	13	80	167	2.053	1.2	0.1811	0.50	2663	17	2558	49	96
33	–	2	9	34	114	3.195	1.1	0.1205	0.90	1964	32	1756	34	89
34	–	2	9	41	107	2.507	1.1	0.1520	0.50	2369	17	2164	42	91
35	–	4	18	69	220	3.089	1.1	0.1142	0.50	1868	18	1808	36	97
36	–	4	20	73	254	3.381	1.3	0.1134	0.73	1855	26	1670	39	90
37	–	26	107	429	1337	2.996	1.1	0.1157	0.50	1891	18	1857	36	98
38	–	3	11	57	133	2.262	1.2	0.1635	0.50	2492	17	2360	47	95
39	–	3	9	52	118	2.198	1.2	0.1651	0.50	2509	17	2417	48	96
40	–	17	72	284	894	3.046	1.2	0.1137	0.50	1860	18	1830	38	98
41	–	6	29	106	367	3.365	1.2	0.1101	0.50	1801	18	1677	35	93
42	–	3	14	56	172	2.992	1.2	0.1127	0.50	1843	18	1859	37	101
43	–	2	8	32	105	3.156	1.1	0.1115	0.55	1824	20	1774	35	97
44	–	10	43	173	531	2.976	1.1	0.1591	0.50	2446	17	1868	36	76
45	–	3	14	55	173	3.059	1.2	0.1131	0.50	1850	18	1823	38	99
46	–	1	8	25	104	3.982	1.4	0.1047	0.81	1709	30	1444	36	85
47	–	15	66	248	827	3.196	1.2	0.1139	0.50	1862	18	1755	37	94
48	–	4	17	62	211	3.270	1.2	0.1103	0.50	1804	18	1720	35	95
49	–	4	13	67	157	2.274	1.2	0.1592	0.50	2447	17	2350	45	96
50	–	6	28	106	346	3.153	1.2	0.1131	0.50	1850	18	1776	38	96
51	–	13	62	226	776	3.288	1.2	0.1127	0.50	1843	18	1712	35	93
52	–	15	62	253	780	2.986	1.2	0.1243	0.50	2018	18	1862	38	92
53	–	3	8	45	97	2.075	1.3	0.1940	0.50	2776	16	2535	53	91
54	–	3	10	56	127	2.190	1.2	0.1636	0.50	2494	17	2424	48	97
55	–	1	5	21	67	3.061	1.2	0.1132	0.78	1852	28	1822	37	98
56	–	6	24	95	297	3.002	1.3	0.1136	0.50	1857	18	1853	42	100
57	587	3	18	58	225	3.738	1.4	0.1423	0.81	2256	28	1528	39	68
58	–	4	17	64	217	3.225	1.2	0.1150	0.50	1879	18	1741	37	93
59	–	10	40	165	504	2.944	1.2	0.1187	0.50	1936	18	1885	38	97
60	–	5	23	86	284	3.148	1.2	0.1118	0.50	1828	18	1778	37	97
61	–	5	16	88	206	2.239	1.1	0.1583	0.50	2438	17	2380	45	98
62	–	6	23	106	286	2.429	2.1	0.1461	1.11	2301	38	2222	80	97
63	–	5	14	83	171	1.969	1.1	0.1839	0.50	2689	17	2648	49	98
65	–	10	30	162	372	2.227	1.2	0.1752	0.50	2608	17	2391	50	92
666	–	5	20	83	253	2.935	1.2	0.1185	0.50	1934	18	1890	41	98
67	–	11	41	181	506	2.676	1.2	0.1357	0.50	2174	17	2047	41	94
68	–	8	24	140	305	2.077	1.2	0.1657	0.50	2515	17	2533	50	101
69	–	7	31	123	390	3.091	1.4	0.1137	0.50	1859	18	1807	43	97
70	–	7	26	117	328	2.664	1.3	0.1253	0.50	2033	18	2055	45	101
71	–	6	19	99	239	2.335	1.2	0.1587	0.55	2442	19	2298	47	94
73	–	4	18	71	219	2.922	1.1	0.1136	0.50	1857	18	1898	37	102
74	–	6	28	106	351	3.219	1.2	0.1114	0.50	1822	18	1744	38	96
75	–	3	15	58	184	3.043	1.2	0.1138	0.50	1861	18	1832	39	98
76	–	5	19	87	242	2.674	1.2	0.1280	0.50	2071	18	2048	43	99
77	–	18	76	306	951	2.994	1.2	0.1197	0.50	1951	18	1858	40	95
78	–	5	20	79	249	3.006	1.3	0.1145	0.50	1872	18	1851	41	99
79	–	3	10	51	123	2.318	1.2	0.1615	0.50	2471	17	2312	47	94
80	–	7	29	122	362	2.809	1.3	0.1190	0.50	1941	18	1963	44	101
82	327	12	61	209	760	3.485	1.2	0.1101	0.50	1801	18	1626	35	90
84	–	5	18	83	221	2.579	1.3	0.1513	0.50	2360	17	2112	48	89
85	–	1	4	17	53	3.004	1.2	0.1141	0.95	1866	34	1853	38	99
86	339	9	40	152	505	3.180	1.3	0.1174	0.50	1917	18	1763	41	92
87	–	24	76	404	948	2.245	1.2	0.1604	0.50	2460	17	2375	47	97
88	–	16	70	273	868	3.022	1.2	0.1130	0.50	1848	18	1843	38	100
89	–	8	33	130	413	3.024	1.2	0.1129	0.50	1846	18	1842	39	100
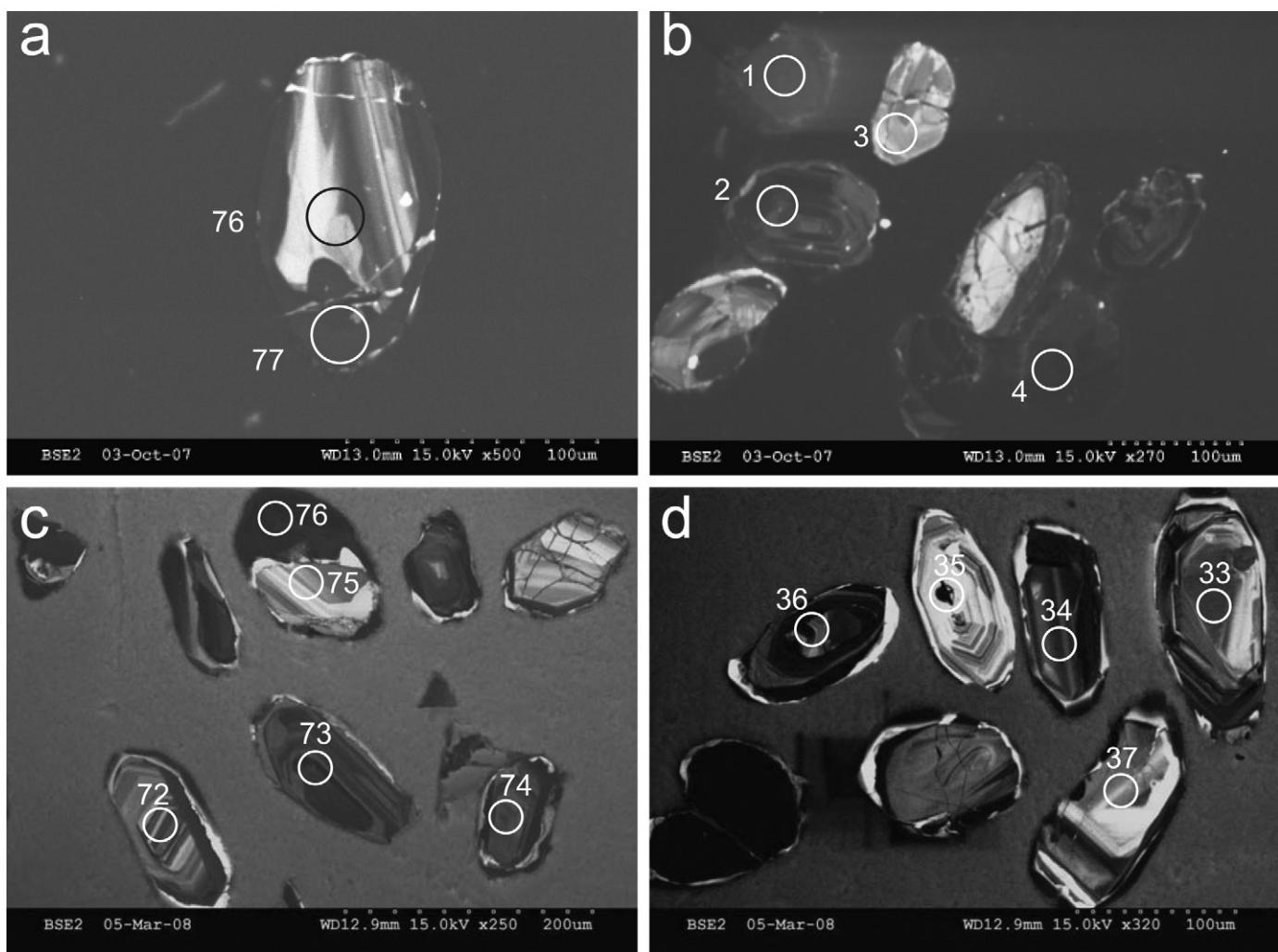
Fig. 7. Cathodo-luminescence imagery of selected zircon grains from samples of the Maha Group; sample CP183b (a, b) and sample PP727 (c, d).

uncertainty of the data point $^{207}Pb/^{206}Pb$ ages of 19 Ma (2σ) and a histogram bin width efficiency of 82.7% (at 40 Ma bin width). The probability density distribution indicates age maxima at: 2690, 2660, 2640, 2510, 2480, 2450, 2380, 2300, 2070, 2030, 1940 and 1860 Ma (Fig. 6d) rounded to the nearest 10 Ma (Fig. 8b). Maxima within uncertainty define age ranges of 2690–2640, 2510–2450 and 2070–2030 Ma. The largest mode is that at 1860 Ma which comprises 22 of the 47 concordant data points. The $^{207}Pb/^{206}Pb$ age of the youngest detrital zircon is 1804 ± 18 Ma (2σ), which provides a maximum age of deposition for the sediment. Rim analysis 77 is characterised by high U (951 ppm) and provides an age of 1951 ± 18 Ma (2σ) and possibly records a metamorphic event affecting the source rock prior to incorporation into the quartzite. We note, however, that this analysis may have incorporated core material and therefore represent a mixed age.

Sample PP727 was taken from outcrops of garnet-bearing quartzite, interbanded on a cm- to dm-scale with kyanite-garnet-biotite gneiss located within the MDZ – see sample location on Fig. 3. 91 analyses were conducted on a variety of grains (Fig. 7c and d), of which 39 are within 100 ± 5% concordant (Fig. 8c). Several severely discordant data points indicate some Mesoarchaean components, but based on the most concordant $^{207}Pb/^{206}Pb$ data only, a mean uncertainty of the data point ages of 15 Ma (2σ) and a histogram bin width efficiency of 81.8% (at 30 Ma bin width), the probability density distribution indicates age maxima at: 2770, 2720, 2630, 2590, 2520, 2490, 2160, 1940,

1920, 1870, 1860, 1850 and 1840 Ma (Fig. 8d) rounded to the nearest 10 Ma. Maxima within uncertainty define age ranges of 2520–2490, 1940–1920 and 1870–1840 Ma. The largest mode is that at 1870–1840 Ma which comprises 19 of the 39 concordant data points. The youngest concordant detrital zircon grain yielded a $^{207}Pb/^{206}Pb$ age of 1797 ± 18 Ma, which records the maximum age of deposition of the quartzite agreeing well with that from sample CP183b. A metamorphic rim on one zircon grain was large enough to allow a determination (analysis 76), and yielded a near-concordant $^{206}Pb/^{238}U$ age of 531 ± 8 Ma (106% concordant), which is taken to be a good approximation for the timing of its crystallisation (Table 6). This rim analysis is characterised by a high U content of 1433 ppm, which together with its CL-unzoned nature (Fig. 7c), suggests that it grew during a late Neoproterozoic metamorphic event, probably associated with the emplacement of late tectonic granites at this time.

4.4. Itremo Group

The two samples of Itremo Group rocks that were analysed were collected from within the Ikalamavony Sub-domain of the Itremo-Ikalamavony Belt (Fig. 3). Quartzite sample PF06035 was collected from a narrow unit infolded with marbles and amphibolites in the Itremo-Ikalamavony Domain in the southwestern parts of the Bekodoka Inlier (Figs. 2 and 3). The quartzite sample contained abundant zircon with a wide variety of shapes from transparent

Table 6

Zircon U–Pb LA-MC-ICP-MS data for sample PP727.

Spot	^{204}Pb (cps)	^{206}Pb (mV)	^{238}U (mV)	Pb (ppm)	U (ppm)	^{238}U/^{206}pb	ls%	^{207}pb/^{206}pb	ls%	^{207}pb/^{206}pb	2s abs	^{206}Pb/^{238}U	2s abs	%C
3	–	13	25	101	343	3.011	0.8	0.1139	0.50	1862	18	1849	26	99
5	504	8	15	58	215	3.155	0.9	0.1111	0.50	1817	18	1775	27	98
1	–	3	6	68	231	3.373	0.9	0.1114	0.50	1822	18	1674	26	92
2	–	3	8	61	294	4.714	2.5	0.1078	1.09	1763	40	1240	56	70
3	–	4	7	86	260	3.122	1.0	0.1152	0.50	1884	18	1791	30	95
4	–	3	6	72	220	3.175	0.9	0.1146	0.50	1873	18	1765	28	94
5	–	3	6	61	225	3.613	1.1	0.1099	0.54	1798	19	1575	31	88
6	–	11	13	254	492	1.918	1.1	0.3143	0.50	3542	15	2705	47	76
7	–	7	15	150	559	3.490	0.9	0.1099	0.50	1797	18	1624	26	90
8	417	5	8	117	281	2.301	1.0	0.1619	0.50	2476	17	2326	39	94
11	–	16	26	365	958	2.557	1.1	0.1561	0.50	2414	17	2128	39	88
12	–	7	14	162	499	3.005	1.1	0.1205	0.58	1964	21	1852	35	94
14	–	2	5	55	185	3.233	1.5	0.1471	0.60	2312	21	1738	45	75
16	–	7	15	168	547	3.078	0.8	0.1127	0.50	1843	18	1814	25	98
17	–	5	10	113	367	3.067	0.9	0.1183	0.50	1930	18	1819	27	94
18	–	10	21	229	788	3.225	0.9	0.1132	0.50	1852	18	1741	28	94
19	–	15	20	338	720	1.969	0.8	0.1933	0.50	2770	16	2648	34	96
20	–	7	10	161	368	2.116	0.8	0.1735	0.50	2592	17	2494	33	96
21	–	7	9	156	319	1.928	0.8	0.1870	0.50	2716	16	2694	34	99
22	–	8	17	189	628	3.164	0.8	0.1123	0.50	1836	18	1770	25	96
23	–	4	6	95	221	2.255	0.8	0.1679	0.50	2536	17	2366	32	93
24	–	3	5	60	171	2.626	1.5	0.1673	0.94	2531	31	2080	53	82
25	–	4	7	95	250	2.444	1.2	0.1617	0.50	2473	17	2211	45	89
26	–	11	19	258	699	2.495	1.1	0.1526	0.50	2375	17	2172	39	91
33	–	6	8	136	305	2.069	0.8	0.1669	0.50	2527	17	2541	33	101
34	–	6	10	134	369	2.509	0.8	0.1349	0.50	2163	17	2163	29	100
35	–	3	5	70	192	2.544	1.2	0.1558	0.61	2410	21	2137	45	89
36	–	11	25	246	937	3.395	1.6	0.1268	1.27	2055	45	1664	47	81
37	–	4	6	92	225	2.260	0.8	0.1618	0.50	2475	17	2362	32	95
39	–	3	5	75	170	2.123	0.8	0.1654	0.50	2511	17	2488	33	99
40	–	4	7	92	268	2.592	0.9	0.1351	0.50	2166	17	2103	31	97
41	–	16	28	373	1031	2.474	0.8	0.1556	0.50	2409	17	2188	31	91
42	–	5	9	115	336	2.615	1.1	0.1460	0.65	2299	22	2088	40	91
45	–	6	9	144	328	2.097	0.8	0.1684	0.50	2542	17	2514	33	99
46	–	3	5	69	183	2.431	0.9	0.1581	0.50	2436	17	2221	32	91
47	–	7	16	169	583	3.056	1.2	0.1575	0.56	2429	19	1825	39	75
48	–	8	21	186	766	3.703	0.8	0.1108	0.50	1813	18	1541	23	85
49	–	8	17	193	627	3.023	0.8	0.1188	0.50	1938	18	1842	26	95
50	–	4	8	86	284	3.037	0.8	0.1125	0.50	1840	18	1835	25	100
51	–	4	9	102	334	3.034	0.8	0.1141	0.50	1866	18	1837	25	98
52	–	2	5	50	185	3.325	0.8	0.1099	0.50	1798	18	1695	24	94
53	–	13	41	317	1211	3.728	0.9	0.1070	0.50	1750	18	1532	24	88
54	–	3	8	64	228	3.489	0.9	0.1066	0.52	1742	19	1624	26	93
55	–	16	43	382	1274	3.238	0.8	0.1115	0.50	1824	18	1735	25	95
56	–	6	19	142	572	3.628	1.8	0.1117	0.69	1826	25	1569	51	86
58	–	22	70	542	2080	3.645	0.9	0.1290	0.50	2084	18	1563	24	75
59	–	14	32	333	945	2.738	0.9	0.1511	0.50	2358	17	2007	29	85
60	–	4	9	87	270	3.031	0.9	0.1125	0.50	1841	18	1838	29	100
61	–	21	59	516	1738	3.240	1.2	0.1129	0.50	1846	18	1734	37	94
62	–	5	9	122	267	1.913	2.4	0.2695	0.93	3303	29	2711	106	82
63	314	6	15	136	450	3.140	1.1	0.1125	0.50	1840	18	1782	33	97
64	–	10	21	232	618	2.481	1.0	0.1570	0.50	2423	17	2183	36	90
65	318	2	4	52	119	2.084	0.9	0.1633	0.50	2490	17	2527	36	101
66	–	9	25	210	747	3.283	0.8	0.1099	0.50	1797	18	1714	23	95
68	–	8	16	192	459	2.239	0.8	0.1620	0.50	2477	17	2380	31	96
69	–	15	42	354	1254	3.266	0.8	0.1253	0.50	2033	18	1722	24	85
70	–	10	30	238	887	3.419	1.0	0.1258	0.50	2040	18	1654	30	81
71	–	6	17	156	514	3.042	0.8	0.1140	0.50	1864	18	1832	25	98
72	–	4	8	103	242	2.190	0.8	0.1636	0.50	2493	17	2425	31	97
73	–	17	34	406	1019	2.294	0.8	0.1614	0.50	2470	17	2332	31	94
74	–	6	18	157	530	3.088	0.8	0.1128	0.50	1844	18	1808	24	98
75	–	2	5	37	135	3.365	0.8	0.1093	0.71	1787	26	1677	24	94
76	–	5	48	110	1433	11.658	0.8	0.0573	0.50	501	22	531	8	106
A	–	5	13	89	15	3.135	0.9	0.1131	0.50	1850	9	1785	28	96
B	–	2	5	28	5	3.714	1.2	0.1072	0.73	1753	27	1537	33	88
C	–	2	3	26	3	2.370	0.9	0.1612	0.50	2469	17	2269	34	92
E	–	7	20	120	23	3.557	1.5	0.1081	0.50	1768	9	1597	42	90
G	–	5	11	77	13	3.167	0.9	0.1117	0.50	1827	10	1769	27	97
H	–	3	8	53	9	3.177	0.9	0.1134	0.50	1854	14	1764	27	95
J	–	6	10	99	11	2.118	0.8	0.1666	0.50	2524	6	2493	33	99
K	–	2	6	36	6	3.238	0.8	0.1120	0.50	1833	18	1735	24	95
L	–	1	4	23	4	3.351	0.9	0.1107	0.76	1811	28	1684	27	93
N	–	7	16	112	18	3.042	0.9	0.1176	0.50	1920	7	1832	30	95
O	–	3	8	45	9	3.815	1.1	0.1028	0.52	1675	19	1501	29	90
P	–	19	43	303	48	2.910	1.5	0.1122	0.50	1836	4	1904	48	104
Q	–	7	15	111	17	2.905	1.2	0.1146	0.50	1874	7	1907	41	102

Table 6 (Continued)

Spot	^{204}Pb (cps)	^{206}Pb (mV)	^{238}U (mV)	Pb (ppm)	U (ppm)	$^{238}U/^{206}Pb$	ls%	$^{207}Pb/^{206}Pb$	ls%	$^{207}Pb/^{206}Pb$	2s abs	$^{206}Pb/^{238}U$	2s abs	%C
T	–	3	8	49	9	3.351	0.8	0.1178	0.50	1923	14	1683	25	88
U	–	3	6	49	7	2.501	1.9	0.1568	0.50	2422	11	2169	69	90
V	–	1	2	14	2	2.477	1.3	0.1594	0.88	2449	30	2186	46	89
w	–	10	22	162	25	2.872	1.3	0.1327	0.50	2134	4	1926	42	90
X	–	5	9	75	10	2.512	0.9	0.1581	0.50	2436	7	2160	33	89
Y	–	6	17	104	19	3.411	1.2	0.1105	0.50	1808	8	1657	36	92
z	–	3	9	53	11	3.677	0.9	0.1075	0.50	1757	14	1551	24	88
AA	–	19	45	302	50	3.045	1.2	0.1140	0.50	1865	5	1831	37	98
AB	–	4	6	61	7	2.061	0.9	0.1773	0.50	2628	7	2550	38	97
AC	–	2	6	40	7	3.033	0.8	0.1139	0.50	1863	16	1837	25	99
AD	–	2	6	38	6	3.135	0.9	0.1125	0.52	1841	19	1785	29	97
AF	–	3	9	52	10	3.561	1.0	0.1125	0.50	1840	13	1595	28	87
AH	–	10	14	155	15	1.852	0.9	0.2383	0.50	3109	7	2783	38	90
Al	–	4	10	63	11	3.158	0.8	0.1121	0.50	1834	13	1774	25	97
AJ	–	3	5	52	6	2.130	0.8	0.1638	0.50	2495	10	2481	34	99

euhedral to subhedral tabular grains with well preserved crystal terminations, to brown strongly altered, mechanically rounded fractured grains and angular grain fragments (Fig. 9a, Table 2). In CL, the clear zircon are high U, zoned grains similar to those found in the leucosomes of the Neoarchaean-Early Palaeoproterozoic migmatitic orthogneisses of the Betsiboka Suite of the Antananarivo Craton (CGS, 2009b). Most of the remainder of the zircon have moderate U contents with concentric zoning. Several of the grains have thin low U metamorphic growth rims.

Sixty-two spots were analysed on 60 grains (Table 7) by SHRIMP. Of these, 22 were more than 5% discordant (Fig. 10a). Assessment of "concordant' data indicates a mean uncertainty of the data point common-Pb corrected $^{207}Pb/^{206}Pb$ ages of 49 Ma (2σ) and a histogram bin width efficiency of 75.9% (at 80 Ma bin width). The prob-
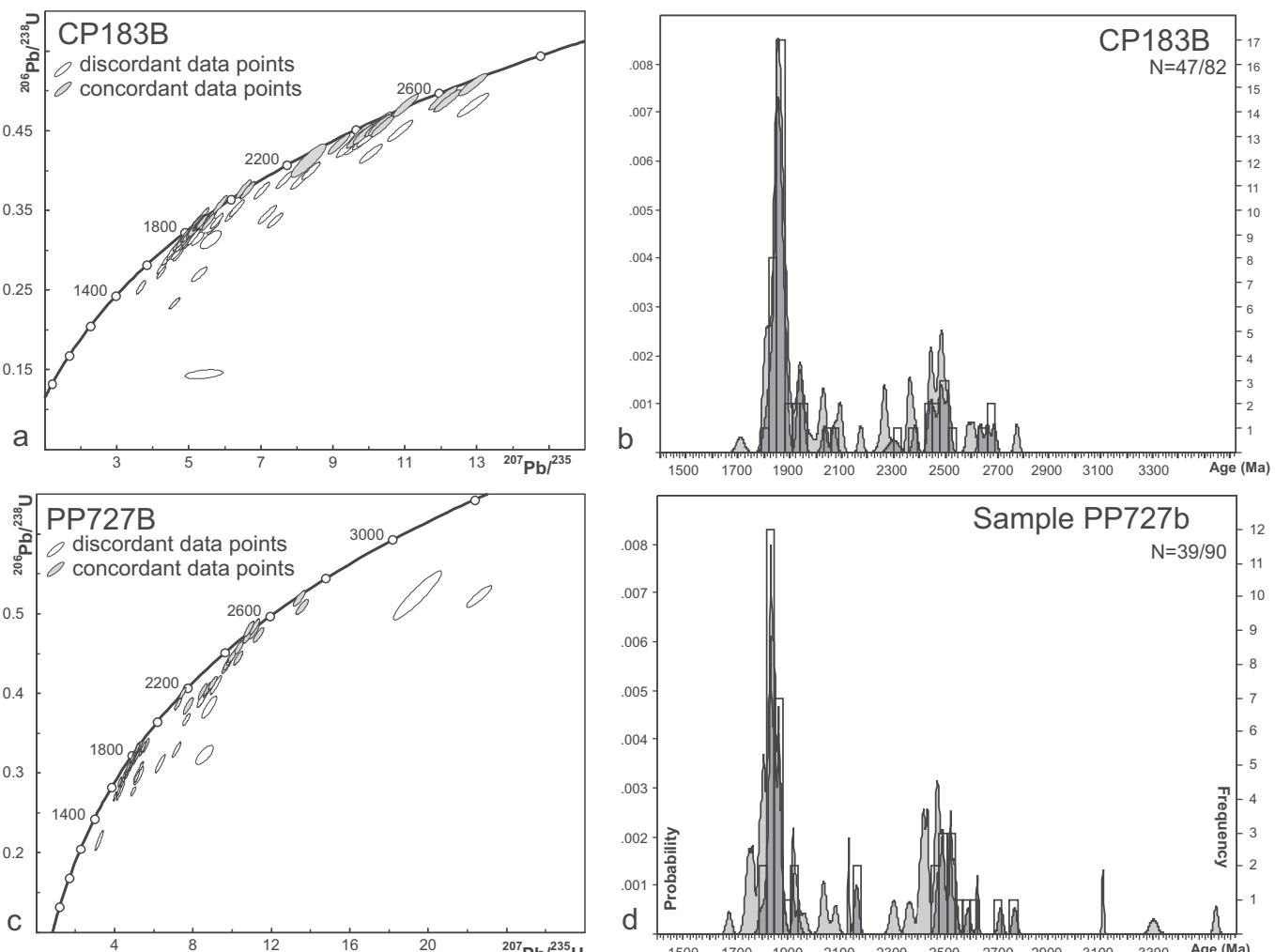
Fig. 8. Plots for LA-MC-ICP-MS zircon U–Pb data for samples from the Maha Group; (a) and (b) Wetherill plot and combined probability-density/histogram plot for sample CP183b; (c) and (d) Wetherill plot and combined probability-density/histogram plot for sample PP727. Uncertainty ellipses are shown at 2σ confidence level. Histogram bin-size is 40 million years for CP183b and 30 million years for PP727 (only 100 ± 5% concordant data are shown in the histogram).
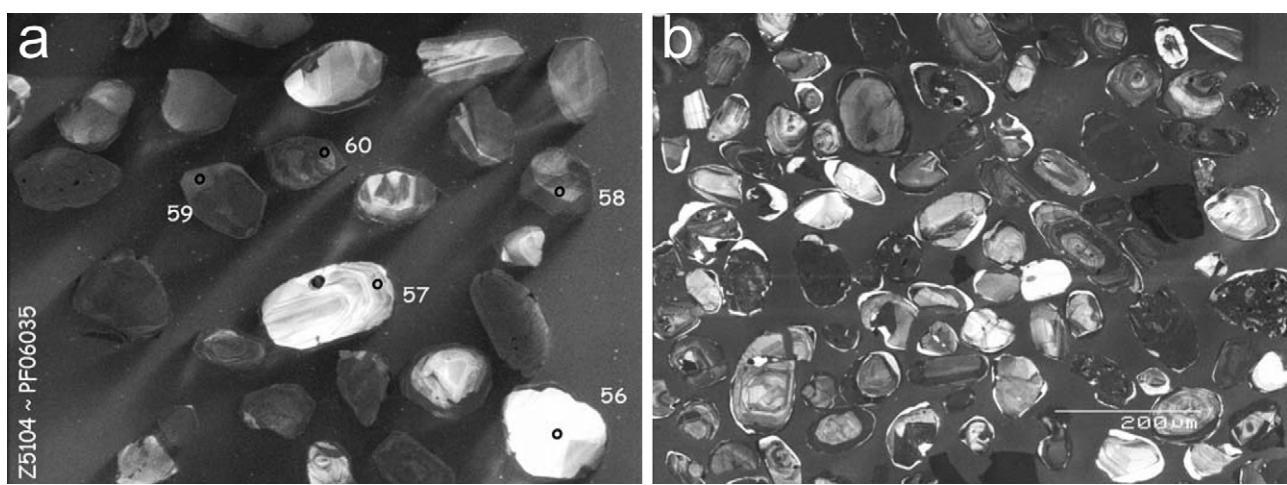
Fig. 9. Cathodo-luminescence imagery of selected zircon grains from samples of the Itremo Group; sample PF06035 (a) and sample PR06088 (b).

ability density distribution indicates age maxima at: 3040, 3000, 2770, 2700, 2610, 2500, 2420, 2170, 2070, 2000, 1920, 1860, 1780, 1470 and 800 Ma rounded to the nearest 10 Ma (Fig. 10b). Maxima within uncertainty define age ranges of 3040–3000, 2770–2700,

2500–2420 and 2070–1780 Ma. The largest mode is that at 2500 Ma with 10 of the 40 concordant data points. Material at 1800–1900 Ma is present but appears more subordinate, but due to the lack of data points for this sample quantitative proportion assessments
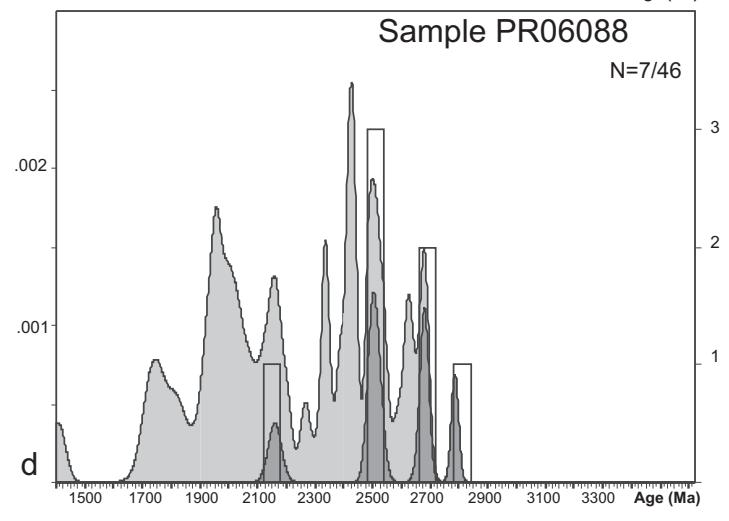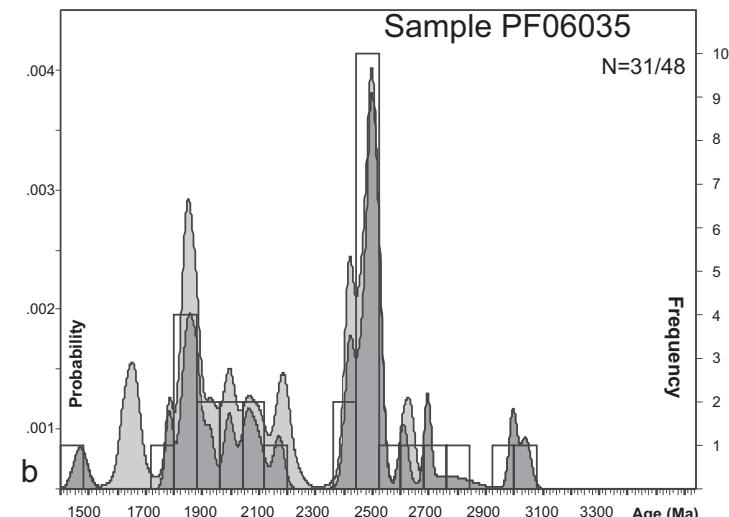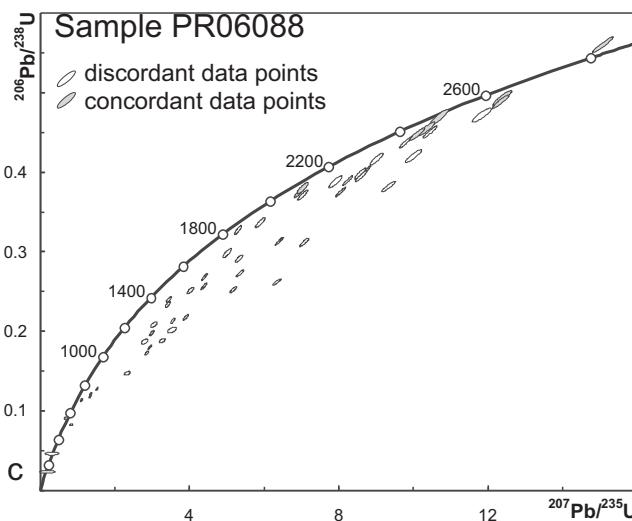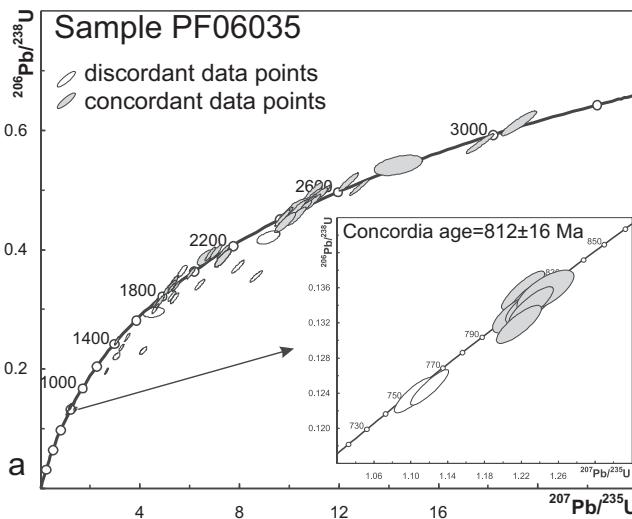
Fig. 10. Plots for SHRIMP zircon U–Pb data for samples from the Itremo Group; (a) and (b) Wetherill plot and combined probability-density/histogram plot for sample PF06035; (c) and (d) Wetherill plot and combined probability-density/histogram plot for sample PR06088. Uncertainty ellipses are shown at 2σ confidence level. Histogram bin-size is 80 million years for PF06035 and 60 million years for PR06088 (only $100 \pm 5\%$ concordant data are shown in the histogram).

Table 7
Zircon U–Pb SHRIMP data for sample PF06035.

Spot name	f_{206} (%)	U (ppm)	Th (ppm)	^{232}Th/^{238}U (ppm)	^{238}U/^{206}Pb (1σ abs err)	^{207}Pb/^{206}Pb (1σ abs err)	^{206}Pb/^{238}U age (2σ abs err (Ma))	^{207}Pb/^{206}Pb age (2σ abs err (Ma))	C%
35-1.1	0.06	570	128	0.23	8.0917 ± 0.0904	0.06397 ± 0.00075	752 ± 15	766 ± 28	98
35-1.2	0.11	45	28	0.64	2.6131 ± 0.0445	0.13494 ± 0.00259	2097 ± 56	2212 ± 33	95
35-10.1	0.08	100	65	0.67	3.0125 ± 0.0418	0.11040 ± 0.00193	1852 ± 41	1842 ± 26	101
35-11.1	0.01	120	83	0.72	1.7368 ± 0.0227	0.22068 ± 0.00165	2935 ± 57	2995 ± 13	98
35-12.1	–	233	159	0.71	2.0294 ± 0.0256	0.16625 ± 0.00158	2583 ± 50	2522 ± 15	102
35-13.1	0.08	1347	309	0.24	8.3286 ± 0.0901	0.06799 ± 0.00066	731 ± 14	873 ± 23	84
35-14.1	–	750	177	0.24	7.3638 ± 0.0821	0.06618 ± 0.00073	820 ± 17	785 ± 27	104
35-14.2	–	313	162	0.54	2.8884 ± 0.0353	0.11351 ± 0.00130	1916 ± 38	1852 ± 22	103
35-15.1	0.15	1043	201	0.20	8.9853 ± 0.0983	0.06501 ± 0.00070	682 ± 14	841 ± 29	81
35-16.1	0.00	416	167	0.41	2.3902 ± 0.0275	0.15776 ± 0.00285	2256 ± 42	2444 ± 58	92
35-17.1	–	166	107	0.67	2.1419 ± 0.0284	0.16339 ± 0.00168	2472 ± 50	2499 ± 18	99
35-18.1	0.03	426	64	0.16	3.9845 ± 0.0450	0.10092 ± 0.00076	1445 ± 29	1659 ± 20	87
35-19.1	–	215	116	0.56	2.5301 ± 0.0320	0.13655 ± 0.00142	2145 ± 43	2170 ± 19	99
35-2.1	0.26	466	230	0.51	3.2976 ± 0.0453	0.14360 ± 0.00698	1656 ± 34	1858 ± 126	89
35-20.1	0.04	493	95	0.20	3.0968 ± 0.0343	0.12833 ± 0.00088	1789 ± 34	1957 ± 21	91
35-21.1	–	506	40	0.08	2.9607 ± 0.0325	0.11419 ± 0.00084	1876 ± 35	1866 ± 26	101
35-23.1	0.02	666	158	0.25	7.4752 ± 0.0843	0.06605 ± 0.00083	810 ± 17	828 ± 29	98
35-24.1	–	284	29	0.11	2.7642 ± 0.0321	0.11426 ± 0.00094	1991 ± 39	1873 ± 28	106
35-25.1	0.02	196	116	0.61	2.1388 ± 0.0275	0.15962 ± 0.00153	2475 ± 49	2460 ± 17	101
35-26.1		286	130	0.47	2.9726 ± 0.0376	0.12819 ± 0.00289	1886 ± 38	2193 ± 18	86
35-26.2		120	55	0.47	1.8504 ± 0.0253	0.19316 ± 0.00484	2785 ± 59	2768 ± 80	101
35-27.1	–	206	278	1.39	2.0452 ± 0.0287	0.16679 ± 0.00304	2565 ± 50	2520 ± 20	102
35-28.1	0.07	1087	105	0.10	7.1415 ± 0.0772	0.06751 ± 0.00065	849 ± 17	984 ± 29	86
35-29.1	–	128	72	0.59	2.0582 ± 0.0282	0.16246 ± 0.00183	2555 ± 54	2490 ± 20	103
35-3.1	0.17	206	89	0.45	3.1387 ± 0.0381	0.12778 ± 0.00123	1776 ± 36	2012 ± 24	88
35-30.1	0.29	501	199	0.41	2.8477 ± 0.0334	0.17170 ± 0.00141	1952 ± 37	2636 ± 15	74
35-31.1	–	585	146	0.26	7.4631 ± 0.0849	0.06639 ± 0.00083	811 ± 17	824 ± 39	98
35-32.1	–	645	152	0.24	7.4224 ± 0.0861	0.06571 ± 0.00079	815 ± 17	810 ± 29	101
35-33.1	–	427	275	0.67	2.0849 ± 0.0246	0.16354 ± 0.00135	2525 ± 46	2489 ± 13	101
35-34.1	–	489	58	0.12	7.3839 ± 0.0869	0.06564 ± 0.00068	820 ± 18	827 ± 48	99
35-35.1	–	195	154	0.81	2.1919 ± 0.0289	0.15618 ± 0.00189	2424 ± 48	2419 ± 17	100
35-36.1	–	227	142	0.65	2.0888 ± 0.0260	0.16623 ± 0.00149	2521 ± 48	2518 ± 15	100
35-37.1	–	68	29	0.43	2.2596 ± 0.0374	0.15791 ± ±0.00193	2369 ± 62	2467 ± 27	96
35-38.1	–	191	123	0.66	1.9500 ± 0.0252	0.17531 ± 0.00163	2669 ± 52	2609 ± 16	102
35-39.1	–	663	154	0.24	7.5963 ± 0.0856	0.06617 ± 0.00078	798 ± 16	838 ± 31	95
35-4.1	0.02	304	94	0.32	2.9996 ± 0.0345	0.11402 ± 0.00086	1857 ± 36	1882 ± 15	99
35-4.2	0.04	159	94	0.61	3.2170 ± 0.0484	0.11280 ± 0.00197	1744 ± 42	1839 ± 26	95
35-40.1	–	439	89	0.21	4.4178 ± 0.0524	0.12293 ± 0.00159	1327 ± 27	2123 ± 33	63
35-41.1	0.00	308	112	0.38	2.9721 ± 0.0355	0.11338 ± 0.00104	1869 ± 37	1847 ± 19	101
35-42.1	–	377	50	0.14	2.7865 ± 0.0316	0.12263 ± 0.00066	1977 ± 38	1994 ± 17	99
35-43.1	–	102	18	0.19	2.5979 ± 0.0363	0.12391 ± 0.00172	2101 ± 49	2029 ± 49	104
35-44.1	–	512	62	0.13	4.5628 ± 0.0508	0.10029 ± 0.00166	1280 ± 25	1658 ± 56	77
35-45.1	0.07	1117	129	0.12	7.7537 ± 0.0846	0.07255 ± 0.00180	788 ± 16	1185 ± 57	67
35-46.1	0.01	691	73	0.11	4.2870 ± 0.0464	0.10057 ± 0.00080	1354 ± 26	1660 ± 22	82
35-47.1	–	85	34	0.41	1.6381 ± 0.0236	0.22676 ± 0.00166	3076 ± 68	3039 ± 20	101
35-48.1	0.22	1389	56	0.04	7.1757 ± 0.0756	0.07089 ± 0.00056	841 ± 16	957 ± 26	88
35-49.1	–	281	200	0.73	2.1250 ± 0.0265	0.16006 ± 0.00234	2485 ± 47	2452 ± 39	101
35-5.1	0.00	67	93	1.42	2.2112 ± 0.0371	0.15975 ± 0.00397	2416 ± 56	2501 ± 22	97
35-50.1	–	675	18	0.03	2.9682 ± 0.0317	0.11838 ± 0.00058	1871 ± 35	1925 ± 17	97
35-53.1	–	242	133	0.57	2.5566 ± 0.0322	0.12716 ± 0.00142	2128 ± 43	2059 ± 20	103
35-54.1	–	274	118	0.45	2.2135 ± 0.0301	0.15672 ± 0.00130	2403 ± 52	2419 ± 15	99
35-55.1	0.06	691	86	0.13	5.1859 ± 0.0581	0.09532 ± 0.00070	1142 ± 23	1624 ± 18	70
35-56.1	–	105	58	0.56	2.0202 ± 0.0289	0.16105 ± 0.00174	2591 ± 57	2463 ± 22	105
35-57.1	0.04	152	90	0.61	2.5337 ± 0.0344	0.12922 ± 0.00175	2146 ± 46	2097 ± 23	102
35-58.1	–	484	49	0.10	1.9853 ± 0.0233	0.18507 ± 0.00067	2629 ± 50	2695 ± 11	98
35-59.1	–	341	57	0.17	7.5265 ± 0.0902	0.06488 ± 0.00094	806 ± 18	819 ± 45	98
35-6.1	0.02	203	183	0.93	2.1033 ± 0.0267	0.16352 ± 0.00197	2509 ± 47	2498 ± 12	100
35-60.1	–	712	259	0.38	3.2405 ± 0.0362	0.10893 ± 0.00091	1734 ± 32	1783 ± 13	97
35-7.1	0.05	162	152	0.97	2.7142 ± 0.0364	0.15380 ± 0.00230	2027 ± 41	2415 ± 17	84
35-8.1	0.06	399	58	0.15	3.3433 ± 0.0369	0.11309 ± 0.00065	1686 ± 32	1843 ± 19	92
35-9.1	0.00	762	186	0.25	8.0321 ± 0.0896	0.06485 ± 0.00070	757 ± 15	783 ± 23	97
35-9.2	0.03	209	127	0.63	4.0878 ± 0.0512	0.08986 ± 0.00162	1414 ± 29	1470 ± 24	96

Analyses were conducted during one session, with standard analyses yielding a 2σ error of the mean of 0.28%. f_{206} = the proportion of common ^{206}Pb in the total ^{206}Pb; Th/U = ^{232}Th/^{238}U; C% = concordance; all ratios and ages are corrected for common Pb using measured ^{204}Pb and composition appropriate to the age of the zircon (Stacey and Kramers, 1975).

are limited. The oldest concordant grain is 3039 ± 40 Ma (2σ). One analysis on a core of a complex zircon yielded a ^{207}Pb/^{206}Pb age of 1470 ± 48 Ma (2σ, 96% concordance) with a second spot on a high uranium rim (metamorphic) overgrowth giving a ^{206}Pb/^{238}U age of 757 ± 30 Ma (2σ, 97% concordance). We interpret this core analysis to either reflect mixing between an older core and the younger rim, or to perhaps date the maximum age of deposition. Apart from this single analysis, the youngest concordant core ^{207}Pb/^{206}Pb age was recorded at 1783 ± 26 Ma (2σ, 97% concordance), constraining the maximum age of deposition for the sample. The clear high U zoned zircons yielded ages between 2450 and 2500 Ma and confirm that the Betsiboka Suite orthogneisses (Antananarivo Domain) represent their most probable source.

Table 8
Zircon U–Pb SHRIMP data for sample PR06088.

Spot name	f_{206} (%)	U (ppm)	Th (ppm)	$^{232}Tn/^{238}U$ (ppm)	$^{238}U/^{206}Pb$	$^{207}Pb/^{206}Pb$	$^{206}Pb/^{238}U$ age	$^{207}Pb/^{206}Pb$ age	C%
					1σ abs err		1σ abs err		
PR06088-1.1	0.05	174	59	0.35	2.6354 ± 0.0321	0.17384 ± 0.00124	2081 ± 41	2631 ± 16	79
PR06088-2.1	–	545	181	0.34	2.5697 ± 0.0282	0.15380 ± 0.00083	2119 ± 38	2387 ± 12	89
PR06088-3.1	0.02	355	235	0.68	2.2919 ± 0.0275	0.16209 ± 0.00143	2336 ± 43	2485 ± 12	94
PR06088-4.1	–	143	70	0.51	2.6439 ± 0.0353	0.13214 ± 0.00159	2073 ± 44	2160 ± 23	96
PR06088-5.1	–	139	31	0.23	2.1253 ± 0.0269	0.18068 ± 0.00135	2489 ± 51	2672 ± 22	93
PR06088-6.1	0.51	491	75	0.16	4.1989 ± 0.0469	0.10255 ± 0.00080	1381 ± 27	1719 ± 28	80
PR06088-7.1	0.55	865	361	0.43	5.4103 ± 0.0622	0.11884 ± 0.00209	1103 ± 22	2067 ± 42	53
PR06088-8.1	0.14	158	89	0.58	3.3967 ± 0.0455	0.11436 ± 0.00202	1677 ± 36	1996 ± 27	84
PR06088-9.1	0.25	1501	233	0.16	7.9340 ± 0.0836	0.08915 ± 0.00064	765 ± 15	1409 ± 25	54
PR06088-10.1	0.03	177	84	0.49	2.7082 ± 0.0345	0.13446 ± 0.00147	2033 ± 42	2202 ± 19	92
PR06088-11.1	0.01	608	274	0.47	3.1997 ± 0.0361	0.15016 ± 0.00100	1751 ± 33	2335 ± 11	75
PR06088-12.1	0.07	83	55	0.69	2.1366 ± 0.0321	0.16349 ± 0.00221	2479 ± 57	2511 ± 23	99
PR06088-13.1	0.14	1234	247	0.21	8.6179 ± 0.0924	0.08405 ± 0.00101	708 ± 14	1307 ± 40	54
PR06088-13.2	0.04	136	82	0.62	2.0338 ± 0.0277	0.18098 ± 0.00178	2581 ± 54	2675 ± 17	97
PR06088-14.1	0.00	226	78	0.36	3.0664 ± 0.0374	0.11785 ± 0.00113	1820 ± 37	1929 ± 19	94
PR06088-15.1	0.02	504	359	0.74	2.4932 ± 0.0293	0.15675 ± 0.00145	2176 ± 40	2433 ± 10	89
PR06088-16.1	0.03	578	156	0.28	2.6711 ± 0.0294	0.15655 ± 0.00071	2049 ± 38	2415 ± 10	85
PR06088-17.1	0.84	598	182	0.31	4.7167 ± 0.0547	0.11403 ± 0.00171	1262 ± 25	2119 ± 25	60
PR08066-18.1	–	210	114	0.56	2.0500 ± 0.0256	0.18273 ± 0.00135	2563 ± 50	2683 ± 13	96
PR08066-19.1	0.52	510	167	0.34	4.3284 ± 0.0496	0.10206 ± 0.00115	1347 ± 26	1752 ± 28	77
PR08066-20.1	0.80	635	175	0.28	5.1088 ± 0.0572	0.10872 ± 0.00122	1155 ± 23	1820 ± 32	63
PR08066-21.1	0.00	155	71	0.47	2.5892 ± 0.0356	0.14675 ± 0.00166	2109 ± 47	2328 ± 25	91
PR08066-22.1	0.46	480	54	0.12	3.9913 ± 0.0439	0.11837 ± 0.00092	1440 ± 28	1916 ± 30	75
PR08066-23.1	0.76	1192	85	0.07	8.9623 ± 0.0953	0.07248 ± 0.00082	683 ± 14	1027 ± 47	66
PR08066-24.1	1.24	915	368	0.41	7.1192 ± 0.0858	0.08700 ± 0.00350	875 ± 17	1924 ± 70	45
PR08066-25.1	0.39	324	31	0.10	3.4371 ± 0.0389	0.13520 ± 0.00094	1643 ± 32	2144 ± 26	77
PR08066-26.1	0.02	232	128	0.57	2.2227 ± 0.0273	0.16818 ± 0.00134	2395 ± 46	2541 ± 13	94
PR08066-27.1	0.36	753	169	0.23	4.7616 ± 0.0524	0.11591 ± 0.00109	1237 ± 24	1993 ± 22	62
PR08066-28.1	5.83	1615	206	0.13	12.5480 ± 0.1526	0.06628 ± 0.00365	501 ± 11	1147 ± 111	44
PR08066-29.1	0.19	286	21	0.08	8.4916 ± 0.1041	0.07074 ± 0.00138	728 ± 16	1282 ± 51	57
PR08066-30.1	0.55	695	478	0.71	5.7984 ± 0.0720	0.08893 ± 0.00299	1059 ± 21	1955 ± 23	54
PR08066-31.1	0.06	173	90	0.54	2.9843 ± 0.0401	0.12608 ± 0.00172	1866 ± 40	2066 ± 24	90
PR08066-32.1	0.35	628	75	0.12	3.9906 ± 0.0451	0.14704 ± 0.00111	1446 ± 29	2344 ± 19	62
PR08066-32.2	0.77	783	286	0.38	3.8708 ± 0.0436	0.16799 ± 0.00131	1494 ± 28	2622 ± 15	57
PR08066-33.1	0.02	571	73	0.13	3.7514 ± 0.0412	0.11827 ± 0.00065	1526 ± 29	1957 ± 15	78
PR08066-34.1	0.06	122	48	0.41	2.3960 ± 0.0329	0.16820 ± 0.00162	2259 ± 50	2587 ± 20	87
PR08066-35.1	0.74	802	324	0.42	5.8810 ± 0.0671	0.11832 ± 0.00166	1017 ± 20	1990 ± 30	51
PR08066-36.1	0.00	192	142	0.76	2.2391 ± 0.0297	0.16234 ± 0.00190	2384 ± 48	2496 ± 17	96
PR08066-37.1	0.02	204	99	0.50	1.7910 ± 0.0222	0.19269 ± 0.00129	2866 ± 54	2786 ± 13	103
PR08066-38.1	0.03	209	272	1.35	2.6834 ± 0.0402	0.13211 ± 0.00338	2048 ± 44	2165 ± 19	95
PR08066-39.1	1.07	194	45	0.24	5.1128 ± 0.0696	0.10770 ± 0.00274	1176 ± 27	2078 ± 62	57
PR08066-40.1	0.26	553	166	0.31	3.7227 ± 0.0432	0.13158 ± 0.00129	1552 ± 30	2266 ± 18	68
PR08066-41.1	0.23	216	96	0.46	2.4081 ± 0.0297	0.15599 ± 0.00143	2242 ± 44	2428 ± 18	92
PR08066-42.1	0.50	551	200	0.38	3.9056 ± 0.0439	0.12748 ± 0.00097	1466 ± 28	2029 ± 20	72
PR08066-43.1	2.51	400	226	0.58	5.4981 ± 0.0727	0.09238 ± 0.00410	1097 ± 23	1803 ± 61	61
PR08066-44.1	0.07	279	126	0.47	3.2067 ± 0.0442	0.16837 ± 0.00625	1745 ± 35	2513 ± 15	69
PR08066-45.1	0.02	160	132	0.85	2.2132 ± 0.0303	0.16114 ± 0.00226	2413 ± 50	2513 ± 20	96
PR08066-46.1	0.02	349	232	0.69	2.5225 ± 0.0304	0.15445 ± 0.00157	2157 ± 41	2420 ± 16	89
PR08066-47.1	0.16	287	182	0.65	2.5443 ± 0.0314	0.15496 ± 0.00170	2144 ± 41	2439 ± 15	88
PR08066-48.1	0.79	574	287	0.52	4.8997 ± 0.0596	0.09477 ± 0.00192	1213 ± 25	1759 ± 52	69
PR08066-49.1	13.77	36	5	0.13	48.4727 ± 1.9169	0.04201 ± 0.02231	137 ± 16	1083 ± 2449	13
PR08066-50.1	0.74	110	3	0.02	11.1629 ± 0.1590	0.06154 ± 0.00155	552 ± 15	577 ± 197	96
PR08066-51.1	20.72	140	7	0.05	22.7231 ± 0.5779	0.05090 ± 0.01547	279 ± 17	425 ± 1556	66

Analyses were conducted during one session, with standard analyses yielding a 2σ error of the mean of 0.17%. f_{206} = the proportion of common ^{206}Pb in the total ^{206}Pb; Th/U = $^{232}Th/^{238}U$; C% = concordance; all ratios and ages are corrected for common Pb using measured ^{204}Pb and composition appropriate to the age of the zircon (Stacey and Kramers, 1975).

Six data points from analyses of zircon rims cluster around Concordia and give a concordia age of 812 ± 16 Ma (Fig. 10a) with two younger (ca. 750 Ma) near concordant rim ages possibly defining Pb-loss during late-Neoproterozoic reworking.

Quartzite sample PR06088 was collected from a thick quartzite package at the centre of an F_2 dome structure near the western border of the Itremo-Ikalamavony Belt. The strongly recrystallised quartzites are slightly feldspathic with some ferruginous layers. The sample yielded two main groups of small (ca. 100–180 μm) detrital zircons (Table 2, Fig. 9b). Roughly 25% of the zircons are rounded, subhedral to anhedral, caramel-brown crystals with pitted surfaces. The remaining 75% are small rounded to subrounded, colourless transparent ovoid crystals, free of inclusions. The CL images indicate the rock contains a heterogenous array of detrital zircons, but three main morphological groups may be identified (Fig. 9b). The first group represents mechanically rounded fragments of moderate U, concentrically zoned, magmatic zircons. The second group represents moderate U, concentrically zoned magmatic zircons that are not fractured and the third group is characterised by low U unzoned grains. Most grains have thin, unzoned, light-CL (low U) rims, but only one was wide enough to allow analysis.

The 51 zircon grains analysed by SHRIMP yielded a range of strongly discordant data (Fig. 10c, Table 8). Assessment of "concordant' (>95%) data (only 7 data points, excluding 1 younger rim age) indicates a mean uncertainty of the data point common-Pb

Table 9
An overview of age constraints for the Palaeoproterozoic metasedimentary successions of Madagascar. References as follows: (*) this study; (1) Cox et al., 2004a; (2) Buchwaldt et al., 2003; (3) Jöns et al., 2006; (4) BGS-USGS-GLW, 2008; (5) Handke et al., 1999; (6) Fernandez and Schreurs, 2003; (7) Tucker et al., 2007; (8) CGS, 2009a; (9) Thomas et al., 2009.

	Itremo group	Sahantaha group	Maha group
Metamorphic zircon	Ambalavao Suite 550 Ma (1, *)	Maevarano Suite 520 Ma (2, 3)	Ambalavao Suite 530 Ma (4, *)
Oldest intrusive	Imorona-Itsindro Suite ~800 Ma (5, 6, 7)	Antsirable Nord Suite 760 Ma (4, 9)	Imorona-Itsindro Suite ~820 Ma (4)
	Dabolava Suite ~1000 Ma (7, 8)		
Youngest detrital zircon	1720 Ma (1)	1800 Ma (4,*)	1800 Ma (4,*)
Basement rocks	Antananarivo Craton 2500 Ma (7, 8)	Antananarivo and Antongil cratons 2500 Ma and possibly 3200 Ma (4)	Masora Craton 2500 and 3200 Ma

corrected $^{207}Pb/^{206}Pb$ ages of 36 Ma (2σ) and a histogram bin width efficiency of 81.4% (at 60 Ma bin width). The probability density distribution indicates age maxima at: 2790, 2680, 2500 and 2160 Ma rounded to the nearest 10 Ma (Fig. 10d). One analysis on a high uranium unzoned rim yielded a concordant $^{206}Pb/^{238}U$ age of 552 ± 30 Ma (2σ), recording a metamorphic overprint at that time. Due to the strongly discordant nature of these zircon analyses and the few concordant points, no proportional interpretation or constraints on depositional age can be made from these data. However, the concordant ages do still resolve source material of ca. 2790, 2680, 2500 and 2160 Ma contributing to this sample, although other potential ages of source material are not resolvable.

5. Discussion

5.1. Three groups of apparent common provenance

This study shows that lithologically similar metasedimentary rocks of the Itremo, Sahantaha and Maha groups in west-central, northern and east-central Madagascar yield common spectra of detrital zircon ages, and coeval youngest detrital grains (Table 9). Based on the youngest detrital zircon, all three groups were deposited sometime after ca. 1.8 Ga, probably during the Palaeoproterozoic. The Itremo and Sahantaha groups are mainly composed of interlayered quartzites, calc-silicates and metapelites, with a volcanic component (amphibolites) which could not be dated directly. In contrast, the Maha Group is dominated by pelitic rocks associated with quartzites, and with more common amphibolitic rocks. The sedimentary facies in each group varies from proximal shelf (quartzites with or without carbonates) to distal basinal (metapelites, possible metaturbidites). In general, the proximal facies lie adjacent to the present domain margins, suggesting that the units represent dissected remnants of former continental margin successions that were deposited no earlier than ca. 1.8 billion years ago.

5.2. Potential source terranes

Previous workers have suggested that the Itremo Group was originally derived from Palaeoproterozoic provenance areas in East Africa (Cox et al., 2004a; Fitzsimons and Hulscher, 2005), including the 2.0–1.8 Ga Ubendian and Usagaran belts and the ca. 1.8 Ga Muva Supergroup. The abundant presence of 1.8 Ga zircon in the Sahantaha and Maha groups also matches an East African provenance model, but cannot be considered a viable option if we accept the model of a Neoproterozoic suture (the Betsimisaraka Suture), which would have separated the Sahantaha and Maha groups from East Africa during the Palaeoproterozoic

An alternative source of 1.8 Ga zircons is provided by recent work in southern Madagascar that has identified Palaeoproterozoic rocks in the Anoysen-Androyen Domain (2.2–1.8 Ga; Tucker et al., 2010a), which is separated from the Antananarivo Craton by a major shear zone. The occurrence of Dabolava Suite intrusions in

both the Antananarivo and Anoysen-Androyen Domains does indicate that the two domains were linked before 1.0 Ga so that the Palaeoproterozoic rocks of the Anoysen-Androyen Domain could have been a proximal source for the 1.8 Ga detrital zircons in the Itremo sediments. If this linkage occurred prior to deposition of the Itremo, Sahantaha and Maha groups, and if there is no Neoproterozoic suture in East Madagascar, then the 2.2–1.8 Ga rocks within the Anoysen-Androyen Domain could have formed a potential source for all three groups.

Another potential source area for the 1.8 Ga detrital zircons is the Greater Dharwar Craton (Tucker et al., 2010b). This comprised present-day South India and parts of Sri Lanka and possibly either the Antananarivo, Antongil and Masora cratons, or just the Antongil and Masora cratons if the Betsimisaraka Suture exists. The 1.8 Ga rocks identified along the northwestern margin of the Greater Dharwar Craton within the Aravalli Mobile Belt (Roy, 1988; Wiedenbeck and Goswami, 1994; Gupta et al., 1997; Singh et al., 2010; AMB on Fig. 1) could have been the missing proximal source for the Sahantaha and Maha sediments. Limited geochronological data in the Aravalli Mobile Belt indicate granitoid magmatism and felsic volcanism between 2026 and 1723 Ma (Naha and Halyburton, 1974a,b; Choudhary et al., 1984; Naha and Mohanty, 1988; Roy, 1988; Sharma, 1988; Sarkar et al., 1989; Wiedenbeck and Goswami, 1994; Fareeduddin and Kröner, 1998; Kaur et al., 2009; Singh et al., 2010). Palaeoproterozoic mineralisation is indicated by model Pb ages of 1.8 and 1.7 Ga for the Rajpura-Dariba deposits in the Bhilwara Belt and the conformable sediment-hosted sulphide ores at Sawar in the Aravalli Belt respectively (Deb et al., 1989, 2001). In addition to those possible primary source rocks, two sedimentary successions are recognised which contain carbonate (including stromatolites) and pelite, and have been metamorphosed at ca. 1.8 Ga (Deb et al., 1989; Sarkar et al., 1989; Sugden et al., 1990; Verma and Greiling, 1995).

5.3. Were any of the groups tectonically emplaced?

The Sahantaha Group is in tectonic contact with the Anaboriana-Manampotsy Belt and the Antananarivo Craton along the Sandrakota Shear Zone (SSZ, Fig. 2), and is thrust over the Antongil Craton along the Andraparaty Thrust. Nowhere in the modern literature has an unconformable contact been described between Sahantaha Group and Archaean basement, and we therefore support an allochthonous or at least parautochthonous setting for this group. The presence of major recumbent folds (nappes) defined by quartzites in the Sahantaha Group illustrates horizontal tectonic transport (BGS-USGS-GLW, 2008).

The Maha Group is mostly preserved as klippen and synformal infolds that are for the most part tectonically bounded and locally constitute thrust slices within the Masora Craton.

The base of the Itremo Group has been described both as tectonic (e.g. Collins et al., 2000a; Nédélec et al., 2003; Collins, 2006; CGS, 2009a,b) or as unconformable (Cox et al., 2004a). Despite this, there is general agreement that the group underwent extensive east-west shortening which, together with a top-to-the-east

shear sense, led Collins et al. (2000a) to interpret the group as an east-vergent stack of thrust sheets. However, the identification of overturned Itremo Group units below Archaean rocks identical to those of the Antananarivo Craton, as well as the unconformable contacts recognised locally, show that the Itremo Group may have been originally deposited on Antananarivo Craton basement. Based on present knowledge, the Itremo Group is therefore best seen as an autochthonous, locally parautochthonous sequence.

5.4. Minimum age of deposition

The Itremo and Maha groups, along with the surrounding crust, are intruded by the Imorona-Itsindro Suite (840–720 Ma) and the Ambalavao Suite (ca. 550 Ma). The oldest intrusive in the Itremo Group is ca. 800 Ma (Handke et al., 1999) and the oldest intrusive into the Maha Group is ca. 820 Ma (BGS-USGS-GLW, 2008), placing minimum ages on both groups (Table 9). In addition, six zircon rims on detrital zircon of one of our Itremo samples indicate the quartzite was affected by metamorphism at ca. 810 Ma, in keeping with deposition prior to that.

The Sahantaha Group was possibly intruded at ca. 750 Ma, but certainly at ca. 530 Ma by the arc-related Antsirabe-Nord and the post-collisional Maevarano suites respectively (Thomas et al., 2009). Based on this, a minimum age of deposition of 750, or 530 Ma can be proposed.

6. Conclusions

Three regionally separated Palaeoproterozoic metasedimentary successions in Madagascar give similar detrital age patterns and maximum ages of deposition (ca. 1.8 Ga). All these sequences have been strongly affected by late Neoproterozoic-Cambrian tectonism, forming the structural contacts of the successions with the Archaean crustal units of Madagascar, locally as thrust sheets. There is no known local source for the ca. 1.8 Ga detrital zircons that dominate the detrital zircon populations in the four samples from the Sahantaha and Maha groups. However, possible sources are recognised from the Greater Dharwar Craton, and this could support the hypothesis that the Antongil and Masora cratons were joined to the Greater Dharwar Craton prior to late Neoproterozoic-Cambrian orogenesis.

For the Itremo Groups samples there is a proximal source preserved in southern Madagascar (Tucker et al., 2010a). If all of Madagascar's Archaean domains were orginally part of the Greater Dharwar Craton, then the 1.8 Ga detrital zircons in the Itremo Group (as well as in the Sahantaha and Maha groups) could have been sourced from the Anoysen-Androyen Domain of southern Madagascar, as well as from other sources in what are now India and Sri Lanka. The alternative suggestion that Ubendian-Usagaran rocks, in what is now east Africa, sourced the Itremo sediments remains a possibility (Cox et al., 1998, 2004a; and Fitzsimons and Hulscher, 2005).

Appendix A. Supplementary data

Supplementary data associated with this article can be found, in the online version, at doi:10.1016/j.precamres.2011.04.004.

References

Alsac, C., 1963a. Feuille Ankotrofotsy I.49, Dabolava J.49, Anjoma – Ramartina K.49, 1/100 000, Service Géologique de Madagascar.

Alsac, C., 1963b. Etude géologigue et prospection des feuilles au 1:100 000: Ankotrofotsy (I-49); Dabolava (J-49); Anjoma Ramartina (K-49). Service du Bureau Géologique, Antananarivo, Madagascar, pp. 147–157.

Ashwal, L.D. (Ed.), 1997. UNESCO-IUGS-IGCP 348/368 International Field Workshop on Proterozoic Geology of Madagascar—Guidebook to Field Excursions. Gondwana Research Group Miscellaneous Publication, p. 53.

Bertucat, M., Ramarokoto, A., Rakotoarisoa, B., Rakotondratsima, J., 1958. Etude Geologique et prospection des feuilles Ambodinonoka-Vohilava (PQ52) Ampasinambo-Ambodilafa (QR51), Marolambo (R50), Service geologique.

Bésairie, H., 1959. Le socle cristallin de Madagascar. International Geological Congress, pp. 47–62.

Bésairie, H., 1964. Madagascar carte géologique. Service Géolographique a Madagascar, Tananarive.

Bésairie, H., 1969. Déscription géologique du massif ancien de Madagascar. Troisième volume: la région centrale. 1. Le Système du Graphite, Groupe d'Ambatolampy. Documentation du Bureau Géologique. Service Géologique de Madagascar, Tananarive, p. 73.

Bésairie, H., 1970. Déscription géologique du massif ancien de Madagascar. Quatrième volume: la région centrale. 2. Le Système du Vohibory, Série schisto-quartzo-calcaire, Groupe d'Amborompotsy. Documentation du Bureau Géologique. Service Géologique de Madagascar, Tananarive, 177d, 86.

BGS-USGS-GLW, 2008. Revision de la cartographie géologique et minière des zones Nord et Centre de Madagascar (Zones A, B et D). R.M. Key, Pitfield, P.E.J., Thomas, R.J., Annels, R.A., Bauer, W., Burton, B., Conrad, J., Chacksfield, B., De Waele, B., Ford, J., Goodenough, K.M., Hall, M., Hawkins, M., Horstwood, M., Howard, K., Jordan, C., Kusky, T., Lapworth, D., Lidke, D., Peters, S.G., Pouliquen, G., Rakotoson, R.L., Ralison, V., Randriamananajara, T., Scheib, A., Schofield, D.I., Smith, R.A., Styles, M., Taylor, C.D., Tucker, R.D., British Geological Survey Research Report. Republique de Madagascar Ministère de L'energie et des Mines (MEM/SG/DG/UCP/PGRM), p. 1049.

Bousteyak, L., 1970. Stratigraphie des migmatites dans la région d'Anjozorobe. Comité National Malgache de Géologie, Tananarive.

Bousteyak, L., Rakotonanahary, Rakotomandimby, Rakotoarivelo, G., Randrianasolo, L. and Raveloson, A., 1970-72. Carte géologique de Anjialavabe – Doany (VW35). Service géologique de Madagascar, Antananarivo.

Bousteyak, L., 1972. Etude geologique et prospection des feuilles Andapa, Maromimbihy (WXY.36) au 1/100.000, completage des feuilles Doany, Anjialavabe (VW.35) et Ambodisatrana (V.36), Rapport Annuel du Service Géologique, 1972, 1–18.

Bousteyak, L., 1974. Etude Geologique et prospection de la feuille au 1/100.000 Doany W.35, Rapport Annuel du Service Géologique, 1971, 1–18.

Brenon, P., 1951. Carte géologique de Andravory – Sambava (VW 34-35, XY 34-35). 1:100,000, Service Géologique.

Buchwaldt, R., Tucker, R.D., 2001. P-T-time constraints on the metamorphic rocks of North Madagascar and their relevance on the assembly of Gondwanaland. In: Anonymous (Ed.), Geological Society of America, 2001 annual meeting. Geological Society of America (GSA). Boulder, CO, United States, p. 436.

Buchwaldt, R., Tucker, R.D., Dymek, R.F., 2002. Petrogenetic implication of three contrasting terranes in northern Madagascar, Geological Society of America, 2002 Annual meeting. Geological Society of America (GSA), Denver, CO, United States, p. 448.

Buchwaldt, R., Tucker, R.D., Dymek, R.F., 2003. Geothermobarometry and U–Pb Geochronology of metapelitic granulites and pelitic migmatites from the Lokoho region, Northern Madagascar. American Mineralogist 88, 1753–1768.

Buchwaldt, R., 2006. Geology of the Neoproterozoic and Cenozoic rocks of North Madagascar, Ph. D. Dissertation. Washington University, St. Louis, Missouri (USA), p. 397.

CGS, 2009a. Map Explanation of 1:100 000 scale (Zone E) Sheets I46 – Ambararata, J46 – Beopoaka, I47 – Itondy, J47 – Belobaka, K47 – Ambatofotsy, I48 – Miandrivazo, J48 – Betrondro, K48 – Ambatondradama, I49 – Ankotrofotsy, J49 – Dabolava, K49 – Anjoma-Ramartina, L49 – Vasiana, M49 – Ankazomiriotra, N49 – Antsirabe. P.H. Macey, Miller, J.A., Armstrong, R.A., Bisnath, A., Yibas, B., Frost-Killian, S., Chevallier, L., Mukosi, N.C., Cole, J., le Roux, P. and Haddon, I.G. Ministère de L'Energie et des Mines - Project de Gouvernance des Ressources Minérales, Antananarivo, Madagascar and Council for Geoscience, Pretoria, South Africa.

CGS, 2009b. Map Explanation of 1:100 000 scale sheets (Zone F) G41 – Ambohipaky, H41 – Bevary, G42 – Mangoboky, H42 – Bekodoka, G43 – Andolamasa, H43 – Andrafialava and parts of G40 – Ankasaksa, F40 – Saint-Andre, F41 – Betsalampy, H40 – Maroboaly-Sud, I40 – Soalala-Sud, I41 – Andranomavo, F42 – Marovoay Kely, I42 – Mahabe, F43 – Bebao, F44 – Antranogoaika, G44 – Morafeno, I43 – Ampoza, H44- Bemolanga and I44 Makaraingo. P.H. Macey, Miller, J.A., Armstrong, R.A., Ingram, B.A., Bisnath, A., Yibas, B., Frost-Killian, S., Chevallier, L., Finkelstein, J. and Haddon, I.G. Ministère de L'Energie et des Mines – Project de Gouvernance des Ressources Minérales, Antananarivo, Madagascar and Council for Geoscience, Pretoria, South Africa.

Choudhary, A.K., Gopalan, K., Sastry, C.A., 1984. Present status of the geochronology of the Precambrian rocks of Rajasthan. Tectonophysics 105, 131–140.

Collins, A.S., Kröner, A., Razakamanana, T., Windley, B.F., 2000a. The Tectonic architecture of the East African Orogen in Central Madagascar – a structural and geochronological perspective. Journal of African Earth Sciences 30, 21.

Collins, A.S., Kröner, A., Razakamanana, T., Windley, B.F., 2000b. The tectonic architecture of central Madagascar; disentangling the amalgamation Gondwana. In: Skilbeck, C.G., Hubble Thomas, C.T. (Eds.), Understanding Planet Earth; Searching for a Sustainable Future; on the Starting Blocks of the Third milLennium; Abstracts. Geological Society of Australia, Sydney, N.S.W., Australia, p. 2000.

Collins, A.S., Fitzsimons, I.C.W., Hulscher, B., Razakamanana, T., 2003a. Structure of the eastern margin of the East African Orogen in central Madagascar. Precambrian Research 123 (2–4), 111–133.

Collins, A.S., Johnson, S., Fitzsimons, I.C.W., Powell, C.M., Hulscher, B., Abello, J., Razakamanana, T., 2003b. A structural section through the East African belt in central Madagascar, Proterozoic East Gondwana: Supercontinent Assembly, Breakup. In: Yoshida, M., Windley, B.F., Dasgupta, S. (Eds.), Proterozoic East Gondwana: Supercontinent Assembly and Breakup. Geological Society, London, pp. 363–379, Special Publication 206.

Collins, A.S., Kröner, A., Fitzsimons, I.C.W., Razakamanana, T., 2003c. Detrital Footprint of the Mozambique Ocean: U/Pb SHRIMP and Pb Evaporation Zircon Geochronology of Metasedimentary Gneisses in Eastern Madagascar. Tectonophysics 375, 77–99.

Collins, A.S., Pisarevsky, S.A., 2005. Neoproterozoic/Cambrian incorporation of India into Gondwana: the evolution of the circum-Indian Orogens. International Geology Review 71, 229–270.

Collins, A.S., 2006. Madagascar and the amalgamation of Central Gondwana. Gondwana Research 9, 3–16.

Cox, R., Armstrong, R.A., Ashwal, L.D., Wit, M.J.D., 1995. Sedimentology, tectonics and geochronology of Proterozoic shelf sediments of the Itremo Group, central Madagascar: implications for the assembly of East Gondwana. Geological Society of America, Abstracts with Programs, 27: A-161.

Cox, R.M., Armstrong, R.A., Ashwal, L.D., Raoelison, I.L., 1996. The geology of the Itremo Group central Madagascar; deformed remnant of a Proterozoic continental shelf sequence. In: Santosh, M., Yoshida, M. (Eds.), Proceedings of the UNESCO-IUGS-IGCP-368 International Field Workshop on the Proterozoic Continental Crust of Southern India. Gondwana Research Group Miscellaneous Publication. Osaka City University, Department of Geosciences, Faculty of Science, Gondwana Research Group, Osaka, Japan, pp. 86–87.

Cox, R., Armstrong, R.A., 1997. Geochronology and provenance of the Itremo Group, central Madgascar. In: Cox, R., Ashwal Lewis, D. (Eds.), Proceedings of the UNESCO-IUGS-IGCP-348/368 international symposium and field workshop on Proterozoic geology of Madagascar; abstract volume. Gondwana Research Group Miscellaneous Publication. Osaka City University, Department of Geosciences, Faculty of Science, Gondwana Research Group, Osaka, Japan, pp. 13–14.

Cox, R., Armstrong, R.A., Ashwal, L.D., 1998. Sedimentology, geochronology and provenance of the Proterozoic Itremo Group, central Madagascar and implications for pre Gondwana palaeogeography. Journal of the Geological Society 155, 1009–1024.

Cox, R., Coleman, D.S., Wooden, J.L., Chokel, C.B., 2000. SHRIMP data from detrital zircons with metamorphic overgrowths reveal tectonic history of the Proterozoic Itremo Group, central Madagascar. In: Anonymous (Editor), Geological Society of America, 2000 annual meeting. Geological Society of America (GSA). Boulder, CO, United States, 2000.

Cox, R., Coleman, D.S., Wooden, J.L., DeOreo, S.B., 2001. A newly recognised Late Neoproterozoic metasedimentary sequence in Central Madagascar suggests terrane juxtaposition at 560 ± 7 Ma during Gondwana assembly. Geological Society of America Abstracts with Programs, 33: A436.

Cox, R., Coleman, D.S., Raharimahefa, T., Chokel, C.B., Wooden, J.L., White, L.D., 2003. Mesoproterozoic Madagascar-Africa Connection Based on SHRIMP U–Pb Ages of Detrital Zircons from the Itremo Group and Sahantaha Series in Central and Northern Madagascar. Annual meeting Geological Society of America, Seattle, p. 302.

Cox, R., Coleman, D.S., Chokel, C.B., DeOreo, S.B., Wooden, J.L., Collins, A.S., De Waele, B., Kröner, A., 2004a. Proterozoic tectonostratigraphy and paleogeography of central Madagascar derived from detrital zircon U–Pb age populations. Journal of Geology 112, 379–399.

Cox, R., Fernandez, A., Schreurs, G., 2004b. Discussion on tectonic evolution of the Proterozoic Itremo Group metasediments in Central Madagascar. Journal of the Geological Society, London 161, 539–541.

de la Roche, H., 1951. Carte géologique d'Ifanadiana – Mananjary (PQRS52-53). 1:200,000 (Antananarivo: Bureau géologique.).

de la Roche, H., 1953. Étude géologique de la region aurifère de Mananjary. Travaux du Bureau Géologique, Madagascar 49, 94.

Deb, M., Thorpe, R.I., Cumming, G.L., Wagner, P.A., 1989. Age, Source and Stratigraphic Implication of Pb Isotope Data for Conformable, Sediment-hosted, Base Metal Deposits in the Proterozoic Aravalli-Delhi Orogenic Belt, Northwestern India. Precambrian Research 43, 1–22.

Deb, M., Thorpe, R.I., Krstic, D., Corfu, F., Davis, D.W., 2001. Zircon U–Pb and galena Pb isotope evidence for an approximate 1.0 Ga terrane constituting the western margin of the Aravalli-Delhi orogenic belt, northwestern India. Precambrian Research 108, 195–213.

De Waele, B., Horstwood, M.S.A., Bauer, W., Key, R.M., Pitfield, P.E.J., Potter, C.J., Rabarimana, M., Rafahatelo, J.M., Ralison, V., Randriamananjara, T., Smith, R.A., Thomas, R.J., Tucker, R.D., 2008. U–Pb Detrital Zircon Geochronological Provenance Patterns of Supracrustal Successions in Central and Northern Madagascar. Colloquium of African Geology, Hammamat, Tunisia, p. 9.

Dormois, R., 1949. Etude Géologique des feuilles Andavakoera et Vohemar. Rapport Annuel du Service Géologique 1948, 19–28.

Emberger, A., 1955. Les terrains cristallins du pays Betsileo et de ses confins orientaux. Thèse d'Etat Thesis, Université Clermont II, Clermont-Ferrand, France.

Fareeduddin, Kröner, A., 1998. Single zircon age constraints on the evolution of Rajasthan granulite. In: P.B.S. (Ed.), The Indian Precambrian. Scientific Publishers (India), Jodhpur, pp. 547–556.

Fernandez, A., Huber, S., Schreurs, G., Villa, I., Rakotondrazafy, M., 2001. Tectonic evolution of the Itremo Region (Central Madagascar) and implications for Gondwana assembly. Gondwana Research 4 (2), 165–168.

Fernandez, A., Schreurs, G., 2003. Tectonic evolution of the Proterozoic Itremo Group metasediments in central Madagascar. In: Yoshida, M., Windley, B., Dasgupta, S. (Eds.), Proterozoic East Gondwana: Supercontinent Assembly and Breakup. Special Publication of the Geological Society, London, pp. 381–399.

Fernandez, A., Schreurs, G., Villa, I.M., Huber, S., Rakotondrazafy, M., 2003. Age constraints on the tectonic evolution of the Itremo region in Central Madagascar. Precambrian Research 123 (2–4), 87–110.

Fitzsimons, I.C.W., Hulscher, B., 2005. Out of Africa: detrital zircon provenance of central Madagascar and Neoproterozoic terrane transfer across the Mozambique Ocean. Terra Nova 17, 224–235.

Fournié, L., Heurtebize, G., 1963. Géologie de la région Ikalamavony-Ampandramaika-Bekisopa, centre sud de Madagascar. Comité National Malgache de Géologie, Tananarive.

GAF-AG-BGR, 2009. Explanatory notes for the Ikalamavony-Itremo Domain, Central Madagascar. Réalisation des travaux de cartographie géologique de Madagascar, Révision approfondie de la cartographie géologique et minière aux échelles 1/100 000 et 1/500.000 zone Sud. (CARTOSUD). Project de Gouvernance des Ressources Minérales, Contrat No 169/05 DP/MEM/SG/DG/UCP/PGRM, Antananarivo, p. 105.

Goodenough, K.M., Thomas, R.J., De Waele, B., Key, R.M., Schofield, D.I., Bauer, W., Tucker, R., Rafahatelo, J.M., Rabarimanana, M., Ralison, A.V., Randriamananjara, T., 2010. Post-collisional magmatism in the central East African Orogen: the Maevarano Suite of north Madagascar. Lithos 116, 18–34.

Goncalves, P., Nicollet, C., Lardeaux, J.M., 2003. Finite Strain Pattern in Andriamena unit (North-Central Madagascar): evidence for Late Neoproterozoic-Cambrian Thrusting during Continental Convergence. Precambrian Research 123, 135–157.

Goncalves, P., Nicollet, C., Montel, J.M., 2004. Petrology and in-situ U–Th–Pb monazite geochronology of ultra-high temperature metamorphism from the Andriamena mafic unit, north-central Madagascar. Significance of a petrographical PT path in a polymetamorphic context. Journal of Petrology 10, 1923–1957.

Gupta, S.N, Arora, Y.K., Mathur, R.K., Iqbaluddin, Prasad, B., Sahai, T.N., Sharma, S.B., 1997. The Precambrian geology of the Aravalli region, southern Rajasthan and northeastern Gujarat. Memoirs of the Geological Survey of India 123, 262.

Handke, M.J., Tucker, R.D., Hamilton, M.A., 1997a. Age, geochemistry, and petrogenesis of the early Neoproterozoic (800–790 Ma) intrusive igneous rocks of the Itremo region, central Madagascar. In: Cox, R., Ashwal Lewis, D. (eds.), Proceedings of the UNESCO-IUGS-IGCP-348/368 international symposium and field workshop on Proterozoic geology of Madagascar; abstract volume. Gondwana Research Group Miscellaneous Publication 5, pp. 28–29.

Handke, M.J., Tucker, R.D., Hamilton, M.A., 1997b. Early Neoproterozoic (800–790 Ma) intrusive igneous rocks in central Madagascar; geochemistry and petrogenesis. In: Anonymous (Editor), Geological Society of America, 1997 Annual meeting. Abstracts with Programs – Geological Society of America (GSA), Boulder, CO, United States, p. 468.

Handke, M.J., Tucker, R.D., Ashwal, L.D., 1999. Neoproterozoic continental arc magmatism in west-central Madagascar. Geology 27 (4), 351–354.

Hottin, G., 1976. Présentation et essai d'interprétation du Précambrien de Madagascar. Bulletin BRGM Sér. 2 Sect. 4 (2), 117–153.

Huber, S., 2000. Geologie und Geochronologie der Itremo Sedimente im Gebiet des Mont Ibity (Zentral Madagaskar). MSc Thesis, Universität Bern, Bern, Switzerland, p. 97.

Inzana, J., Kusky, T., Higgs, G., Tucker, R., 2003. Supervised classifications of Landsat TM band ratio images and Landsat TM band ratio image with radar for geological interpretations of central Madagascar. Journal of African Earth Sciences 37 (1–2), 59–72.

Jöns, N., Schenk, V., Appel, P., Razakamanana, T., 2005a. Two-stage metamorphic evolution of the Bemarivo Belt (northern Madagascar): constraints from reaction textures and in situ monazite dating, European Geosciences Union 2005. Geophysical Research Abstracts 7, Graz, p. 2.

Jöns, N., Schenk, V., Appel, P., Razakamanana, T., 2005b. P-T evolution of the Bemarivo Belt (northern Madagascar): the final assembly of Gondwana. In: Wingate, M.T.D., Pisarevsky, S.A. (Editors), Supercontinents and Earth Evolution, Geological Society of Australia, Abstracts, vol. 81, p. 103, Fremantle.

Jöns, N., Schenk, V., Appel, P., Razakamanana, T., 2006. Two-stage metamorphic evolution of the Bemarivo Belt of northern Madagascar: constraints from reaction textures and in situ monazite dating. Journal of Metamorphic Geology 24, 329–347.

Joo, J., 1963. Feuille Ambararata I.46, Bepoaka J.46, 1/100 000, Service Géologique de Madagascar.

Jourde, G., Razanakolona, J., Rasamoelina, D., Raveloson, S.A., 1978. Carte géologique de Betsiaka-Antanamboa-Ampisikinana (VWX-32). Service géologique de Madagascar, Antananarivo.

Kaur, P., Chaudhri, N., Raczek, I., Kroner, A., Hofmann, A.W., 2009. Record of 1.82 Ga Andean-type continental arc magmatism in NE Rajasthan, India: insights from zircon and Sm–Nd ages, combined with Nd-Sr isotope geochemistry. Gondwana Research 16, 56–71.

Kröner, A., Windley, B.F., Jaeckel, P., Brewer, T.S., Razakamanana, T., 1999a. Precambrian granites, gneisses and granulites from Madagascar: new zircon ages and

regional significance for the evolution of the Pan-African orogen. Journal of the Geological Society, London 156, 1125–1135.

Kröner, A., Windley, B.F., Jaeckel, P., Collins, A.S., Brewer, T.S., Nemchin, A., Razakamanana, T., 1999b. New zircon ages for Precambrian granites, gneisses and granulites from central and southern Madagascar: Significance for correlations in East Gondwana. Gondwana Research 2 (3), 351–352.

Kröner, A., Hegner, E., Collins, A.S., Windley, B.F., Brewer, T.S., Razakamanana, T., Pidgeon, R.T., 2000. Age and magmatic history of the Antananarivo Block, central Madagascar, as derived from zircon geochronology and Nd isotopic systematics. American Journal of Science 300 (4), 251–288.

Kröner, A., 2001. The Mozambique belt of East Africa and Madagascar: significance of zircon and Nd model ages for Rodinia and Gondwana supercontinent formation and dispersal (Du Toit Memorial Lecture 1999). South African Journal of Geology 104 (2), 151–166.

Ludwig, K.R., 2003. Isoplot/Ex Version 3.00: A Geochronological Toolkit for Microsoft Excel. Berkeley Geochronology Center, Berkeley, CA.

Meert, J.G., Nédélec, A., Hall, C., Wingate, M.T.D., Rakotondrazafy, M., 2001. Paleomagnetism, geochronology and tectonic implications of the Cambrian-age Carion Granite, central Madagascar. Tectonophysics 340, 1–21.

Meert, J.G., Nédélec, A., Hall, C., 2003. The stratoid granites of central Madagascar: paleomagnetism and further age constraints on Neoproterozoic deformation. Precambrian Research 120 (1–2), 101–129.

Moine, B., 1963. Feuille Miandrivazo I.48, Betrondro J.48, Ambatondradama K.48, 1/100 000, Service Géologique de Madagascar.

Moine, B., 1966. Grands traits structuraux du massif schisto-quartzo-calcaire (centre ouest de Madagascar). Compte Rendus Semaine Géologique Madagascar, 93–97.

Moine, B., 1967a. Relations stratigraphiques entre la série < schisto-quartzo-calcaire > et les gneiss environnants (centre ouest de Madagascar). Compte Rendus Semaine Géologique Madagascar, 49–53.

Moine, B., 1967b. Etudes complémentaires dans le massif "schisto-quartzo-calcaire" (région d'Ambatofinandrahana). Rapport Annuel du Service Géologique de Madagascar, 69–82.

Moine, B., 1968a. Relations stratigraphiques entre la série «Schisto-Quartzo-Calcaire» et les gneiss environnants (centre ouest de Madagascar): donées d'une première étude géochimique. Comptes Rendus de la Semaine Géologique 1967, 49–53.

Moine, B. 1968b. Carte Géologique à 1/200,000 du massif schisto–quartzo–dolomitique, region d'Ambatofinandrahana, centre-ouest du socle cristallin 172 du Précambrien de Madagascar. Centre de l'Institut Geographique National a Tanananarive (imprimeur), Sciences de la Terre, Nancy (éditeur).

Moine, B., 1974. Caractères de sédimentation et de métamorphisme des séries précambriennes épizonales à catazonales du centre de Madagascar (Région d'Ambatofinandrahana). Sciences de la Terre, Mémoire, Nancy, p. 293.

Naha, K., Halyburton, R.V., 1974a. Early Precambrian stratigraphy of central and southern Rajasthan, India. Precambrian Research 1, 55–73.

Naha, K., Halyburton, R.V., 1974b. Late stress systems deduced from conjugate folds and kink bands in the "Main Raialo Syncline" Udaipur district, Rajasthan India. Bulletin Geological Society of America 85, 251–256.

Naha, K., Mohanty, S., 1988. Response of basement and cover rocks to multiple deformations a study from the Precambrian of central Rajasthan, western India. Precambrian Research 42, 77–96.

Nédélec, A., Bouchez, J.L., Grégoire, V., 2003. Quartz fabric evidence for early Pan-African penetrative east-directed shearing in the Itremo Supracrustal Group of central Madagascar. Terra Nova 15, 20–28.

Nicollet, C., 1990. Crustal evolution of the granulites of Madagascar. In: Vielzeuf, D., Vidal, P. (Eds.), Granulites and Crustal Evolution. Kluwer Academic Publishers, Dordrecht, pp. 291–310.

Paquette, J.L., Nédélec, A., 1998. A new insight into Pan-African tectonics in the East-West Gondwana collision zone by U–Pb zircon dating of granites from central Madagascar. Earth and Planetary Science Letters 155, 45–56.

Paquette, J.L., Moine, B., Rakotondrazafy, M.A.F., 2003. ID-TIMS using the step-wise dissolution technique versus ion microprobe U–Pb dating of metamict Archean zircons from NE Madagascar. Precambrian Research 121 (1–2), 73–84.

Raharimahefa, T., Kusky, T.M., 2009. Structural and remote sensing analysis of the Betsimisaraka Suture in northeastern Madagascar. Gondwana Research 15, 14–27.

Rakotoarimanana, R.H., 2001. Geology and Petrology of the Dabolava Region, West-Central Madagascar with Emphasis on Granite-Hosted Gold Mineralization. University of Witswatersrand, Johannesburg, p. 89.

Raoelison, I.L., 1997. Structure and Metamorphism of the Itremo Group, central Madagascar. MSc Thesis, Rand Afrikaans University, Johannesburg.

Roy, A.B., 1988. Stratigraphic and tectonic framework of the Aravalli Mountain Range. In: Roy, A.B. (ed.), Memoir of Geological Society of India (Precambrian of the Aravalli Mountain, Rajasthan, India), pp. 33–75.

Sarkar, G., Burman, T.R., Corfu, F., 1989. Timing of continental arc-type magmatism in northwest India: evidence from U–Pb zircon geochronology. Journal of Geology 97, 607–612.

Schofield, D.I., Thomas, R.J., Goodenough, K.M., De Waele, B., Pitfield, P.E.J., Key, R.M., Bauer, W., Walsh, G., Lidke, D., Ralison, A.V., Rabarimanana, M., Rafahatelo, J.-M., Randriamananjara, T., 2010. Geological evolution of the Antongil Craton, NE Madagascar. Precambrian Research 182, 187–203.

Sharma, R.S., 1988. Pattern of metamorphism in the Precambrian Rocks of the Aravalli Mountain Belt. Memoir of Geological Society of India (Precambrian of the Aravalli Mountain, Rajasthan India) 7, 33–75.

Singh, Y.K., De Waele, B., Karmakar, S., Sarkar, S., Biswal, T.K., 2010. Tectonic setting of the Balaram-Kui-Surpagla-Kengora granulites of the South Delhi Terrane of the Aravalli Mobile Belt, NW India and its implication on correlation with the East African Orogen in the Gondwana assembly. Precambrian Research 183, 669–688.

Sircombe, K.N., 2004. Age Display: an EXCEL workbook to evaluate and display univariate geochronological data using binned frequency histograms and probability density distributions. Computers and Geoscience 30, 21–31.

Stacey, J.S., Kramers, J.D., 1975. Approximation of terrestrial lead isotope evolution by a two-stage model. Earth and Planetary Science Letters 26, 207–221.

Sugden, T.J., Deb, M., Windley, B.F., 1990. The tectonic setting of mineralisation in the Proterozoic Aravalli – Delhi orogenic belt, NW India. In: Naqvi, S.M. (Ed.), Precambrian Continental Crust and Its Economic Resources. Elsevier, New York, pp. 367–390.

Thomas, R.J., De Waele, B., Schofield, D.I., Goodenough, K.M., Horstwood, M.S.A., Tucker, R., Bauer, W., Annels, A.E., Howard, K., Walsh, G., Rabarimana, M., Rafahatelo, J.M., Ralison, A.V., Randriamananjara, T., 2009. Geological Evolution of the Neoproterozoic Bemarivo Belt, northern Madagascar. Precambrian Research 172, 279–300.

Tucker, R.D., Ashwal, L.D., Handke, M.J., Hamilton, M.A., Le Grange, M., Rambeloson, R.A., 1999. U–Pb geochronology and isotope geochemistry of the Archean and proterozoic rocks of north-central Madagascar. Journal of Geology 107 (2), 135–153.

Tucker, R.D., Kusky, T.M., Buchwaldt, R., Handke, M.J., 2007. Neoproterozoic nappes and superposed folding of the Itremo Group, west-central Madagascar. Gondwana Research 12 (4), 356–379.

Tucker, R.D., Roig, J.Y., Macey, P.H., Delor, C., Amelin, Y., Armstrong, R.A., Rabarimanana, M., Ralison, A.V., 2010a. A new geological framework for south-central Madagascar and the "out-of-Africa" hypothesis. Precambrian Research 185, 109–130.

Tucker, R.D., Roig, J.Y., Delor, C., Amelin, Y., Goncalves, P., Rabarimanana, M.H., Ralison, A.V., Belcher, R.W., 2010b. Neoproterozoic Extension in the Greater Dharwar Craton: a reevaluation of the "Betsimisaraka Suture" in Madagascar. Canadian Journal of Earth Science 48, 389–417.

Verma, P.K., Greiling, R.O., 1995. Tectonic evolution of the Aravalli orogen (NW India): an inverted proterozoic rift basin? Geologische Rundschau 84, 683–686.

Wiedenbeck, M., Goswami, J.N., 1994. High precision 207 Pb/206 Pb zircon geochronology using a small ion microprobe. Geochimica Et Cosmochimica Acta 58, 2135–2141.

Windley, B.F., Razafiniparany, A., Razakamanana, T., Ackermand, D., 1994. Tectonic framework of the Precambrian of Madagascar and its Gondwana connections – a review and reappraisal. Geologische Rundschau 83, 642–659.